University of Stavanger

Faculty of Science and Technology

MASTER'S THESIS

Study program/ Specialization: Master of Science in Biological Chemistry	Spring semester, 2014. ~~Open~~ / Restricted access
Writer: Tina Marie Monge Are	…… (Writer's signature)
Faculty supervisor: Peter Ruoff External supervisor(s): Irene Tveiterås Øvestad, Stavanger University Hospital	
Thesis title: Expression of microRNA-18a and microRNA-18b in the microenvironment of high-grade Cervical Intraepithelial Neoplasia (CIN2-3)	
Credits (ECTS): 60	
Key words: miR-18a miR-18b Cervical Cancer CIN RT-qPCR CISH	Pages: …… + enclosure: …… Stavanger, …….. Date/year

Abstract

Cervical cancer is ranked as the fourth most common cancer worldwide, and the second leading cause of mortality among young woman 19 – 39 of age. Cervical cancer arises from persistent human papilloma (HPV) infection and may take several years to develop. Because of organized screening a premalignant condition of the disease, Cervical Intraepithelial Neoplasia (CIN), can be detected and treated before it becomes invasive and metastatic. microRNA (miRNA) are defined as a class of small non-coding regulatory RNAs, approximately 22 nucleotides long. The miRNAs interferes with the post-transcriptional regulation of gene expression by base-pairing with the 3`-untranslated region of target messenger RNA. MiR-18a is a member of the miR-17-92 cluster which has been found to be a modulator of effector and memory T-cells. In addition, miR-18a and miR-18b have been found to play a role in development of estrogen receptor alpha (ER-α) negative breast cancer.

The aim of this thesis was to optimize methods for isolation, purification and detection of miR-18a and miR-18b in FFPE cervical specimens. The expression of miR-18a and -18b in persistent HPV-16 positive CIN3 samples and normal cervical samples were compared by the use of RT-qPCR and semi-quantitative scoring with CISH.

We found that miR-18a and miR-18b were highly expressed in CIN3 lesions as compared to normal cervical tissue. This might show that high expression of these miRNAs, is a sign of poor prognosis of a lesion with potential to developing into cancer. A comparison between CD8+ T-cells and miR-18a expression indicated a possible relationship between these cytotoxic T-cells and and the miR-18a.

Table of Contents

Acknowledgement

Several persons have contributed academically and practically to this master thesis. First of all, my gratitude goes to my supervisor Irene Tveiterås Øvestad for her time, valuable input and engagement throughout the learning process of this master thesis. You have really been a true inspiration.

I would also like to thank Emiel Jansson, Marija Kilibarda, Bianca van Diermen Hidle, Melinda Lillesand, Einar Gudlaugsson and Kristin Jonsdottir amongst others for their tremendous help throughout the entire process. To Peter Ruoff, thank you for your help with the administrative tasks.

And Finally, I would to thank my family and Fredrik for their help and patience throughout these intense months.

June 2014

Tina Marie Monge Are

Abbreviations

CD4+ T-cell - T-helper cell

CD8+ T-cell - Cytotoxic T-cell

CDK - Cyclin dependent kinase

CIN - Cervical Intraepithelial Neoplasia

CIS - Carcinoma in situ

CISH - Chromogenic in situ hybridization

DC - Dendritic cell

DNA - Deoxyribonucleic acid

FFPE - Formalin Fixed Paraffin Embedded

H&E – Haematoxylin & Erythrosin staining

HPV - Human papillomavirus

hrHPV - High-risk Human papillomavirus

HSIL - High-grade squamous intraepithelial lesion

ICC - Invasive cervical cancer

IFN-α - Interferon alpha

IFN-β - Interferon beta

IL - Interleukin

IRF-1 - Interferon regulatory factor-1

Ki-67 - Ki-67 protein

LC - Langerhans cell

LCR - Locus control region

LSIL - Low-grade squamous intraepithelial lesion

MHC - Major histocompatibility complex molecule

miR / miRNA - MicroRNA

NK - Natural killer cell

p16 - p16 protein

p53 - Protein p53

pRb - Retinoblastoma protein

RT-qPCR - Real time quantitative polymerase chain reaction

TGF-β - Tumor growth factor beta

Th1 - T-helper cell type 1

Th2 - T-helper cell type 2

TNF - Tumor necrosis factor

UICC - Union for International Cancer Control

WHO - World health organization

1 Introduction

1.1 Cervical Cancer

Cervical cancer arises from persistent human papilloma virus (HPV) infection and may take several years to develop. It is ranked as the fourth most common cancer worldwide, and the second leading cause of mortality among young women 19–39 of age [1, 2]. There has been estimated 528 000 new cases and 266 000 deaths from cervical cancer in 2012. Almost 87 % of the deaths occurred in less developed countries, due to poorly developed screening programs and treatment options (Figure 1) [3]. Despite the high mortality rates, this disease is regarded as one of the most preventable form for cancer due to the possibility of early diagnosis by the use of papanicolaou cervical smears (PAP smears) [4].

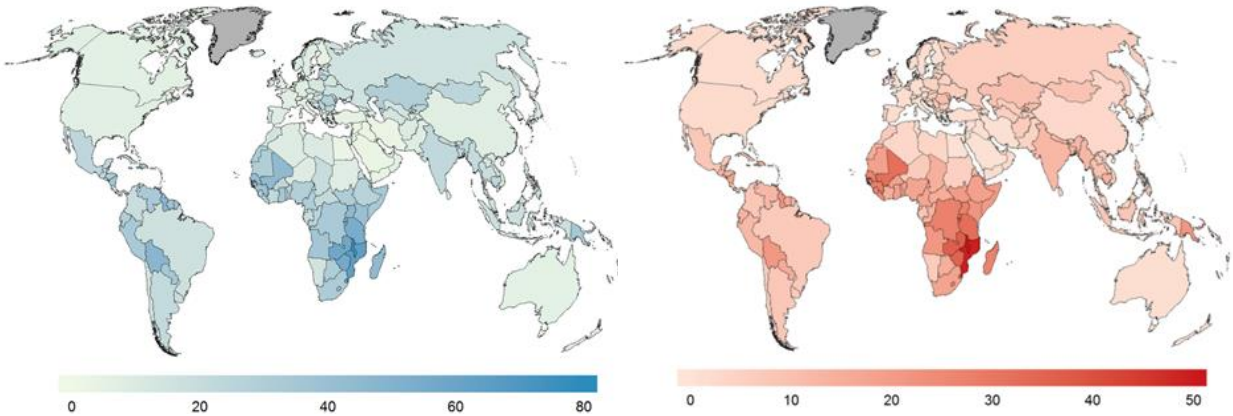

Figure 1. The blue world map show estimated cervical cancer incidence worldwide in 2012 (per hundred thousand). The red world map show estimated cervical cancer mortality worldwide in 2012 (per hundred thousand) [3].

The primary screening method, is used in cancer diagnostics all over the world. It is carried out by taking a PAP smear from the cervix, stain the smear and evaluate it by light microscopy. If abnormal cells are detected, the diagnosis is confirmed by a biopsy before the area is surgically removed by conization. This interrupts the natural course of cervical cancer, thus, stops disease progression [5, 6]

In Finland, Sweden and Iceland, organized screening programs have been carried out since the 1960s. An organized screening program did not start in Norway until November 1994. In the 1970s screening was concentrated on younger women, and mainly spontaneous [7]. In 1990 Union for International Cancer Control (UICC) concluded that to achieve maximum effect of cervical screening, an organized screening program with high coverage in age group 25-60 and screened at 3-5 year intervals should be conducted [8]. Followed by this many countries, including Norway, introduced organized cervical screening with only minor adjustments in the different countries.

The cervix consists of ectocervix and endocervix (Figure 2). The ectocervix is covered by stratisfied squamous epithelium, while the endocervix is lined by mucin producing columnar (also called glandular) epithelium [9]. A ring of tissue overlaps ectocervix and endocervix, this is called the transformation zone. The cells in the transformation zone are constantly changing, making it vulnerable towards an HPV infection [10].

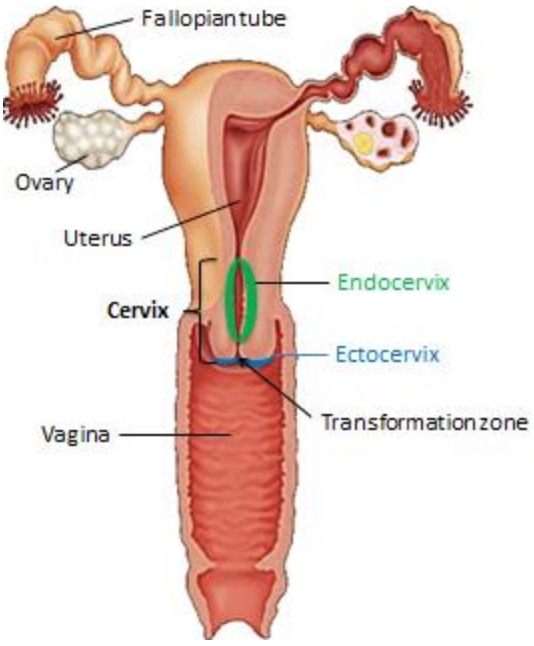

Figure 2. The cervix is located between the vagina and uterus.

Trials which mainly focus on HPV are of great importance. There is now overwhelming evidence that DNA screening is more sensitive than the traditional cytological screening, for detecting pre-malignant conditions of the disease [11, 12]. Furthermore, two vaccines have been developed towards the most aggressive types of HPV (HPV-16 and HPV-18), named

Gardasil (Merck) and GlaxoSmithKline (Cervarix). These vaccines have been available in Norway since 2006-2007 and Gardasil has been included in the Norwegian childhood immunization program for all girls in the 7th grade (age 12 years) [13].

Cytological screening and the use of vaccines have reduced the incidence of cervical cancer in many western countries by almost 80 % [14]. The downward trend is clearly a result of early diagnosis, therapy and vaccination against the HPV virus. Still, there lies a huge challenge in making screening and treatment available to all women at risk, thus, especially within high-risk groups in less-developed countries. Screening and vaccination are two valid approaches, but they require high population coverage, laboratory facilities for screening and diagnostics as well as an organized program [5]. Another possible approach involve a more cost-effective HPV-testing, where the high sensitivity of HPV-DNA testing indicates that only a few screenings are needed during a lifetime [11].

1.1.1 Cervical Intraepithelial Neoplasia

Over 80 % of all cases of cervical cancer are squamous cervical carcinoma, and are preceded by a pre-malignant lesion. The lesion is known as Cervical Intraepithelial Neoplasia (CIN) [15]. Development from CIN to Carcinoma *In Situ* (CIS) is a slow process as average detection age of high grade CIN is 29 years, whereas patients with invasive cancer are 10–20 years older [16].

The lesions are less severe than carcinoma *in situ* due to the lack of capacity to invade the subepithelial stroma [17]. An HPV infection in the cervix produces koilocytosis, followed by a nuclear enlargement and formation of a perinuclear halo in the epithelium. This is typically seen in CIN formation [18]. In 1973 Richart *et al.* proposed that the term Cervical Intraepithelial Neoplasia (CIN) should be used on all cervical precursor lesions, including carcinoma *in situ* to help standardize the treatment of these lesions [19]. This permits grading of the lesions based on how infected cells expand to occupy the upper layers of the epithelium [18].

Today two systems, the CIN system and the Bethesda system, are used in the classification of cervical precursor lesions. The three-tiered CIN system classifies mild dysplasia as CIN1, moderate dysplasia as CIN2 and severe dysplasia as CIN3 [17]. In the two-tiered Bethesda

system (TBS), low-grade squamous intraepithelial lesion (LSIL) represents a HPV infection with relative low risk of progressing to carcinoma *in situ*, while high-grade squamous intraepithelial lesion (HSIL) represents a HPV infection with higher risk of progressing to cervical cancer [20]. The European guidelines recommend that all systems should be translatable into the Bethesda system, and TBS is often used for cytological abnormalities, while the CIN terminology is used for histological lesions [21]. Both LSIL and HSIL correspond to the CIN classification system (Table 1) [16, 22].

Table 1. Combination of the two-tiered Bethesda system and CIN terminology, used throughout the world in classification of pre-malignant cervical lesions.

SIL	LSIL	HSIL
The Bethesda system	Low-grade squamous intraepithelial lesion	High-grade squamous intraepithelial lesion
CIN Terminology	CIN1	CIN2-3
	LSIL corresponds to CIN1	HSIL corresponds to CIN2-3
Dysplasia terminology	Mild dysplasia	Moderate to severe dysplasia

Two biomarkers often used in development and behavior of CIN, are Ki-67 and $p16^{INK4a}$ (p16) [23]. Ki-67 is a marker for proliferation, whilst p16 expression is regulated by a pRb-dependent negative feedback loop. High-risk HPV E7 protein inactivates pRb, thus increasing the levels of p16 [16]. These markers are widely used together with hematoxylin and eosin (H&E) stained sections, to give more accurate results in the grading of CIN.

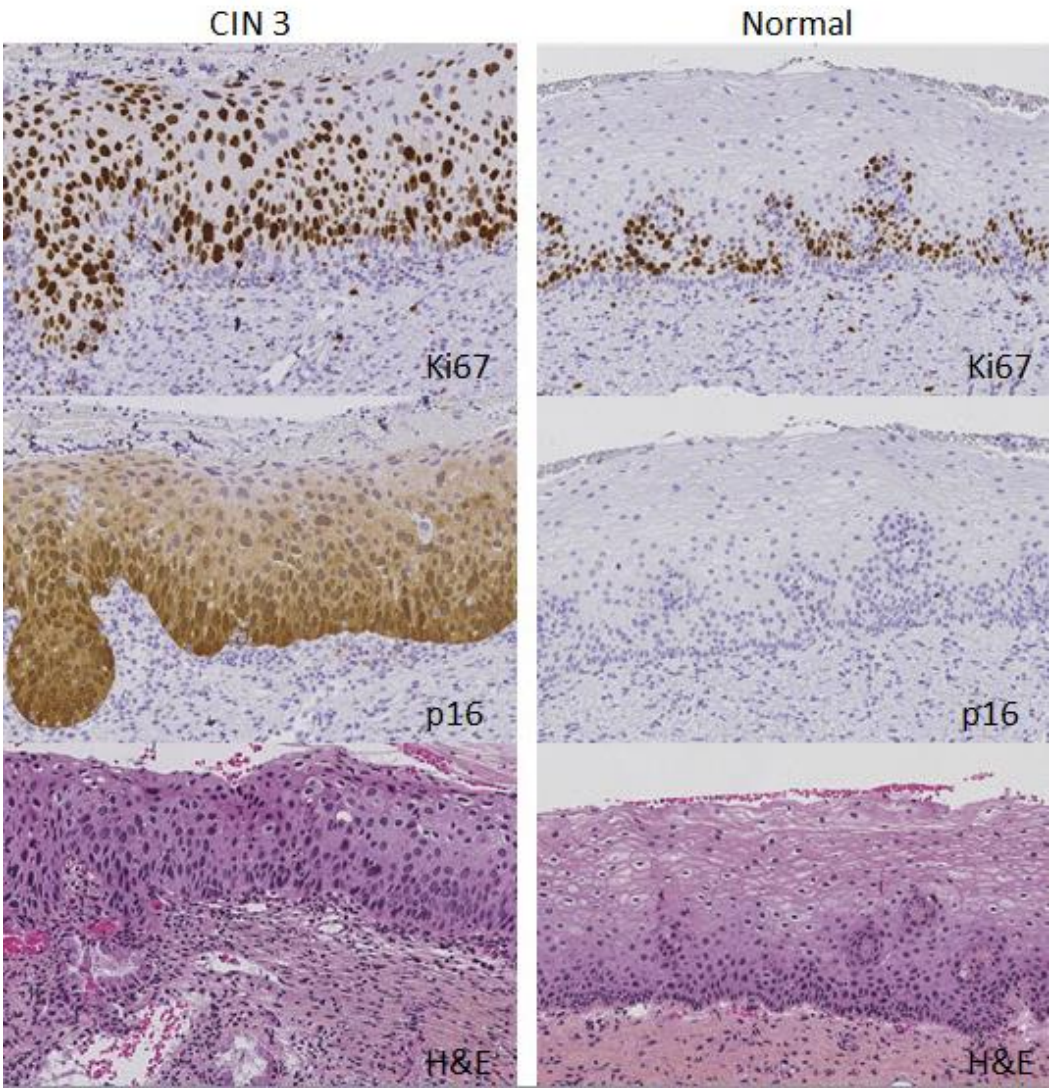

Figure 3. The left figure show CIN3 tissue stained with Ki67, p16 and H&E. Normal cervical tissue is stained with the same biomarkers in the right figure.

The three distinct grades used of CIN (two in SIL), may give the impression of a static process rather than dynamic. However, the process of a pre-malignant lesion is dynamic, whereas it may progress and persist or regress. Thus, CIN2-3 lesions are usually treated with cone excision, even though up to 40 % of CIN2-3 cases may regress spontaneously [24]. This regression may relate to the balance between the genotype of HPV and response of the patient's own immune system [25].

Several risks are associated with surgical removal of CIN. Bleeding complications, preterm delivery, adverse pregnancy and late abortion are some of the major concerns [26, 27]. Studies have shown that there is a significantly increased risk of preterm delivery after

excisional treatment [27, 28]. It is of uttermost importance to develop diagnostic predictive methods to predict the risk of progression and regressions of CIN lesions and in this way, reduce the number of overtreatment [25, 29].

1.1.2 Human Papilloma Virus (HPV)

Papillomaviruses are small non-enveloped DNA viruses, which infect cutaneous and mucosal epithelium in a vast majority of higher vertebrates [30]. The papillomaviruses are specie-specific and human papillomavirus (HPV) will only affect humans [31]. HPV is composed of an 8kb double-stranded (ds) circular genome protected by a viral capsid [9]. More than 150 types of HPV have been identified, whereas 40 are able to infect the cervix [32].

HPV infection is very common and up to 80 % of men and women have been infected with one or several types of genital HPV during their lifetime [31]. The genital types of HPV are divided into high-risk groups and low-risk groups. The low-risk HPV share a common life cycle, but cannot cause neoplasia or carcinoma *in situ* [33]. Genital warts are caused by low-risk HPV (HPV-6 and HPV-11). World Health Organization (WHO) has classified 12 high-risk HPVs (16, 18, 31, 33, 35, 39, 45, 51, 52, 56, 58, 59) and two possible high-risk HPVs (68, 73) which all have the ability to cause cancer [34].

The HPV virus is transmitted through sexual activities and can infect the vaginal, oral and anal epithelium [35]. Sexual behavior such as number of partners, early age of intercourse and the sexual activity span are important factors related to infection of HPV [26]. Condoms offers up to 60 % protection, and it has been shown that condoms may also promote regression of CIN [31]. One possible explanation on why condoms promote regression of CIN might be that the condom reduces exposure of HPV to the cervix, thus, strengthen cellular immune response. Other hypothesis includes semen having an immunosuppressive role and that the latex of the condom stimulates the immune system [26, 36].

The dsDNA genome of HPV encodes a long control region and eight Open Reading Frames (ORFs) [37]. The genome is divided into two main regions; the early region and the late region. The early region encodes for six proteins necessary for viral replication and cell proliferation (E1, E2, E4, E5, E6 and E7). The late region encodes for two proteins (L1 and L2) necessary for creation of the viral capsid. Transcription of genes are controlled by the Locus

Control Region [38]. The papillomavirus life cycle differ from other virus due to its ability to only develop and reproduce in the epidermal or mucosal epithelial cells. The virus invade the basal layer through breaches in the upper layers of the epithelium [39].

The basal layer, which separates the epithelium and stroma, give rise to new cells which differentiates into mature cells while travelling towards the epithelial surface. The basal cells are the only proliferating cells in the epithelium, and HPV is dependent on infecting these cells. During an infection, high-risk HPV genomes are either established as episomal (the virus remains in cytoplasm) or integrated (the viruses genome becomes a part of the host genome) [38, 40]. In normal circumstances, the basal cells will become differentiated and exit the cell cycle in the suprabasal epithelial layer, but with an active HPV infection, the host cell remains active in the cell cycle and continues to replicate while migrating towards the upper layers of the epithelium [41]. The ability of HPV to replicate in the basal cells, without being integrated, is solely dependent on the E1, E2 and E4 protein [37]. E1 and E2 are responsible for the replication and DNA transcription of HPV, whilst E4 is necessary for maturation and release [42].

The oncogenic proteins E5, E6 and E7 are involved in cellular transformation. E5 binds to host growth factor receptors and membrane proteins to enhance amplification of the virus. E5 facilitates the immune system invasion by down-regulating the major histocompatibility complex (MHC) class I molecules, thus, impairing antigens to be presented on the host cell surface [30]. “High-risk” E6 and E7 proteins interfere with the cell cycle control by inhibiting the functions of tumor suppressor proteins p53 and pRb [39].

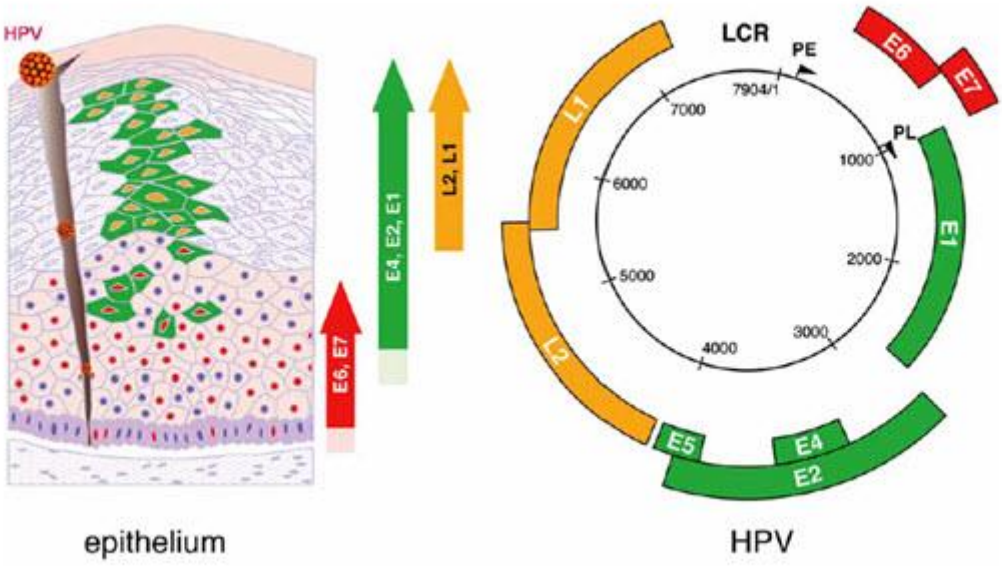

Figure 4. The left figure shows a schematic illustration of how the HPV virus infects the basal layer through wounds in the epithelium. When the basal cells are infected, viral proteins are produced at different times in the life cycle. The right figure show a schematic illustration of the HPVs genome [37, 40].

The oncoprotein E7 binds to the pRB family (p105, p107 or p130) and inhibit their ability to modulate the function of E2F transcription factors. The role of pRB is to prevent the cell from replicating damaged DNA in the cell cycle by controlling the E2F transcription factors [43]. E2F activates cyclin E and c-Myc sequences which are important in further cell proliferation [41].

A p53 dependent pathway is activated by cell proliferation and may inhibit cell growth, induce apoptosis or promote DNA repair to prevent deregulated cell growth. E6 degrades p53 through binding to an ubiquitin ligase (E6-AP), forming a dimer that binds to p53. p53 is ubiquitinated, recognized by the proteasome and degraded. In this way the host cell may replicate continuously with the possibility for inducing neoplasia and cancer [44]. In a low risk HPV infection, E6 and E7 will not stimulate cell proliferation [34]. During the life cycle process the HPV genome sometimes is integrated into the host genome leading to the loss of parts of the HPV genome. The result of this integration is an uncontrolled upregulation of E6 and E7 oncogenic proteins and continuous uncontrolled proliferation of the host cell [10].

The HPV life cycle is adapted to evade a host immune response. Even though the HPV invades the basal layer it does not fully replicate until the host cell reaches the superficial epithelium. Because of the short life span of the host cells, apoptosis is naturally induced in this layer [45]. This is part of the healthy cell maintenance and the newly synthesized virus can exit the cell without inducing cellular responses or inflammation [46].

The HPV can delay or inhibit the hosts immune response by inhibiting the host cells synthesis of IFN-α, IFN-β, macrophage inflammatory protein 3a and tumor necrosis factor (TNF) [47]. For example, E7 oncoprotein can bind to Interferon-Regulator Factor-1 (IRF-1) and downregulate IFN-α [25]. Normally the host cell produces antigens which react with major histocompatibility complex (MHC) class I or II. MHC class I molecules are recognized by cytotoxic T-cells (CD8+ T-cells) and MHC class II molecules are recognized by T-helper cells (CD4+ T-cells) [25]. CD4+ T-cells develop into Th1 and Th2 helper cells and secrete cytokines that activate Interferons (IFN), macrophages, NK cells, CD8+ T-cells and B-lymphocytes to produce antibodies [48].

1.2 microRNA

RNA, along with DNA and proteins, defines the major biological macromolecules that are essential for all known forms of life. The main types of RNA are messengerRNA (mRNA), ribosomalRNA (rRNA) and transferRNA (tRNA). mRNA serves as a template for translation of genetic instructions into proteins. Functional or non-coding RNA molecules are transcribed from a DNA sequence, but are not translated into a protein. These RNA molecules include rRNA, tRNA and other small RNAs [49].

In 1993 Lee and colleagues discovered two small temporal RNAs called lin-4 transcripts, involved in developmental timing in *Caernohabidits elegans*. These transcripts consisted of 22 and 61 nucleotides (nt) and are complementary to the 3' untranslated region of lin-14 messenger RNA. The hypothesis was that lin-4 regulated the translation of lin-14 mRNA by interacting via RNA-RNA binding [50]. Seven years later, another small temporal RNA of similar size was discovered by Reinhart *et al*. This small RNA, called let-7, was also involved in developmental timing of *C. elegans* [51]. Within the following year homologs of the *let-7* gene were identified in other animals, including humans. The small temporal RNAs were

named microRNAs (miRNAs / miRs), and the discovery of their regulatory function has led to an enormous interest in miRNA studies [52]. miRNAs are defined as a class of small non-coding regulatory RNAs, approximately 22 nucleotides long [15]. The miRNAs are complementary or partly complementary to mRNA molecules and interferes with the post-transcriptional regulation of gene expression. This is achieved by base-pairing with the 3`-untranslated region of target mRNA [53, 54]. Each miRNA can bind up to 200 different gene targets and thereby controlling a wide range of biological functions such as cellular proliferation, differentiation, apoptosis, metabolism, viral infection and tumor genesis [55]. Previous studies by Guo *et al.* have revealed that approximately 85 % of mRNA regulation in mammalian cells is due to miRNA interactions [54]. The biogenesis of microRNA involves a three step-wise process (Figure 5) [56].

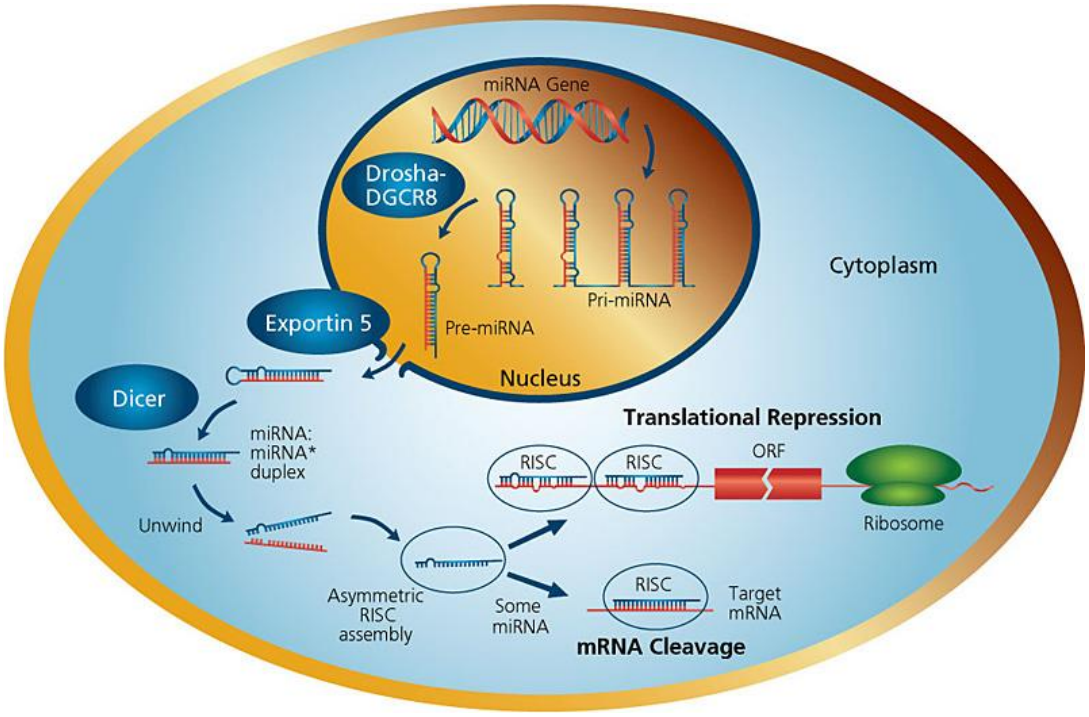

Figure 5. Illustration of the miRNA biogenesis as described above [57].

RNA polymerase II transcribes a large RNA sequence, pri-miRNA, whose tertiary structure forms a stem loop. The pri-miRNA stem loop is cleaved by a microprocessor complex consisting of a ribonuclease RNase III enzyme (Drosha), a RNA binding protein and other factors [58, 59]. This cleavage results in a pre-miRNA, a hairpin shaped RNA molecule of 70-100 base pairs. Pre-miRNA can also be formed directly from the splicing and debranching of

introns in pre-mRNA, thereby, skipping the first step in the miRNA process [60]. A nuclear export receptor, exportin- 5, recognizes the pre-miRNA in nucleus and transport it to the cytoplasm. Once in the cytoplasm, the pre-miRNA is released from the export receptor after hydrolysis of GTP [56]. The pre-miRNA is further processed to mature miRNA by the RNase III enzyme complex, Dicer. Dicer recognizes a 3` overhang of the pre-miRNA with a PAZ domain, and positions itself to cleave the miRNA into double-stranded ~ 22 nt products. This double-stranded miRNA is referred to as microRNA/microRNA* duplex, where the microRNA* strand is unstable and easily degrades. After cleavage by the DICER, the stable strand of the duplex is incorporated into a miRNA-induced silencing complex (miRISC complex). The complex can bind to and regulate the translation of mRNA [56, 61].

1.2.1 miRNA and its role in cancer

Early in the history of miRNA there were suggestions that they played a potential role in human cancer. The first discovered miRNA transcripts, named lin-4 and let-7 in *C. elegans*, and later in *D. melanogaster*, were shown to control both cell proliferation and apoptosis [50]. Later discoveries showed that many of the known miRNA genes are located inside or near fragile sites in the genome, commonly amplified or deleted in human cancer [62]. In 2003 Calin and colleagues found that two miRNA genes, miR-15 and miR-16, were located within a 30-kb deletion on chromosome 13q14. This region was found to be deleted in >65 % of B cell chronic lymphocytic leukemia (B-CLL) cases and the miRNAs were absent or downregulated in 68 % of the CLL cases. This led to the suggestion that these miRNAs were involved in the pathogenesis of CLL [63]. A couple of years later, two independent studies showed relationship between the miRNA cluster, miR-17-92, and expression of MYC [64, 65].

The miR-17-92 cluster is one of the most studied miRNA cluster and has been shown to play an oncogenic role in various cancer types [66]. This cluster can be separated into three miRNA families; the miR-17 family (miR-17, miR-20, miR-18), miR-19 family (miR-19a, miR-19b) and miR-92 family [67]. Overexpression of the miR-17-92 cluster has been found in various cancers including T-cell lymphomas, retinoblastomas, colorectal cancer, head and neck cancer, pancreatic cancer and breast cancer [68]. miR-18a and miR-18b have a crucial role in estrogen receptor alpha (ER-α) negative breast cancer [69, 70]. Highly significant association has been found between high expression of miR-18a and -18b and estrogen

receptor negativity, high proliferation and cytokeratin 5/6 positivity [71]. The miR-17-92 cluster has also been shown to have important roles in other human diseases including neurodegenerative and immune cardiovascular diseases [68].

Many tumor cell lines secrete excess latent Transforming Growth Factor-β (TGF-β1), and resistance to growth inhibitory TGF-β signaling is common. In cervical carcinoma cell lines, levels of latent TGF-β1 correlate inversely with cytostatic response [72]. TGF-β polypeptides are cytokines which play an important role in regulating cells, for instance epithelial and immune cells, by controlling survival processes such as proliferation and differentiation [73]. Latent TGF-β1, miR-18a, miR-24, trombospondin-1 (TSP-1) and FURIN are members of a feedback loop controlling the cytostatic response to TGF-β in HeLa cervical carcinoma cell culture (Figure 6) [74]. Expression of miR-18a and miR-24 are indirectly maintained by high levels of latent TGF-β1, resulting in repression of cytostatic TGF-βs own processing factors, FURIN and TSP-1. Upon TGF-β signaling, miR-18a and miR-24 are inhibited, thus, inducing FURIN and TSP-1 (Figure 6). As a result of increased mature TGF-β processing, caspase 3/7 activation is seen, leading to apoptosis. Reduced processing of latent TGF-β1 precursors and increased TGF-β transcription were also observed [74].

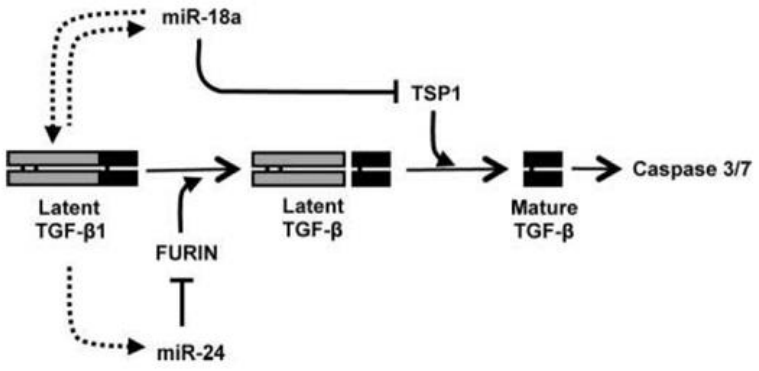

Figure 6. Latent TGF-B1 feeback loop in HeLa cells, indirectly controlled by miR-18a and miR-24 [74].

1.2.2 miRNA in cervical cancer

Several studies have performed miRNA profiling in different stages of cervical cancer development, from normal to high grade cervical neoplasia (CIN2-3) and invasive cancer [15, 75, 76]. Screening of differentially expressed mRNA have identified molecular markers and differentially expressed genes between cervical cancer and normal cervical epithelium [77]. Differences that frequently occur in tumor-specific miRNA signatures, have been traced back to differences in the miRNome (defined as the full complement of miRNA in a genome). This has been detected in in normal versus pathologic cervical tissue [53, 78, 79]. These tumor-specific miRNA signatures can be used to diagnose the origin of the neoplasia and specific tumor subtypes.

By search of literature, different miRNAs affecting development of cervical cancer and high grade CIN have been found to be interesting. In 2012 Cheung *et al.* identified 12 highly upregulated miRNAs in CIN and cervical cancer tissue, as compared to normal cervical epithelium [15]. One of these was miR-34 b/c. The miR-34 family is known to be directed towards p53 target genes and upregulation of miR-34 b/c expression induces cell-cycle arrest, or apoptotic response [80]. Paradoxically, in a group of patients with cervical cancer, transcription of miR-34a was down regulated by HPV oncogenic E6 [79, 81]. In particular, increased levels of miR-25 and miR-92 have been correlated with progression of cervical lesions, making them possible biomarkers of CIN [81]. HPV E6 and E7 oncoproteins are known to deregulate the expression of miR-17-92 cluster, miR-15-16 cluster, and miR-106b-25 cluster via E6/p53 and E7/pRb pathways [79]. The miR-15-16 cluster has also been considered as tumor suppressors due to targeting proteins involved in G1/S checkpoint in the cell cycle [82].

HPV is found in many cases of head and neck squamous cell carcinoma (HNSCC) [83, 84]. HPV positive (+) HNSCC has a distinct miRNA profile that differs from HPV negative (-) HNSCC [83]. There are several similarities between miRNA profile of HPV+ HNSCC and miRNA profile of cervical squamous cell carcinoma (CSCC), in spite of the two different anatomical locations. Especially miR-15a, miR-16, miR-143 and miR-145, are of interest due to their belonging clusters known to have distinct interactions within E6/p53 and E7/pRb viral pathway [79, 82].

Papillomaviruses also encode their own miRNA species, which, in high risk HPV types seems to be involved in cell cycle, immune functions, cell adhesion, migration, development and cancer [85].

Specific miRNA signatures found in CIN and cervical cancer can be used in diagnosis prognosis and response to chemotherapy [53]. Identification of miRNA expression in CIN may contribute to understanding pathogenesis and progression/regression of CIN. In addition, identification of these miRNA expression patterns may be used as therapeutic targets early in the pre-malignant stage [15].

Over the past years, a number of high-throughput approaches have been used to detect and quantify miRNAs in both fresh and Formalin Fixed Paraffin Embedded (FFPE) tissue. Real time quantitative PCR (RT-qPCR) can detect and quantify even small differences in expression of specific miRNAs between samples. Other approaches such as microarrays and northern blotting have also been widely used [56]. Previous studies have also demonstrated that miRNA profiling can provide more accurate classification of human cancers, than mRNA profiling [76, 86].

1.3 Formalin Fixed Paraffin Embedded (FFPE) tissue

FFPE tissue represents an easy way to preserve specimen of interest for longer periods of time. FFPE makes biopsy and autopsy material readily available to molecular analyses such as gene expression analysis [87]. In many countries with cervical cancer screening programs, women with abnormal cytology are referred for colposcopy and a punch biopsy to confirm the presence or absence of high grade neoplasia (CIN2-3). All high grade neoplasia is usually treated surgically by conization. Removed tissue is then fixed in buffered formaldehyde for a certain amount of time (usually 24–48 hours) and embedded in paraffin. Formalin causes cross-linking between nucleic acids and proteins, which preserve the structural integrity and protein structures of a cell and prevent the tissue from degrading. The tissue sections can then be easily deparaffinized in xylene and rehydrated in alcohol prior to the molecular analysis [88]. However, protein cross-linking decreases the efficiency of PCR. Longer fragments of RNA are easily fragmented both during time between surgical removal of the tissue, fixation and during increased storage depending on the pH of the fixative [88, 89].

miRNA has been shown to be more resistant to fragmentation than for instance mRNA [90]. There are many hypothesis as to why miRNA is more stable in FFPE; for instance, their small size; lack of structure; lack of specific target sequence or the fact that they often are found in a protected environment such as the miRISC which may protect them from degrading [89].

1.4 Cresyl violet staining

For better visualization of the cells for light microscopy, different staining methods are used. Cresyl violet is a basic stain which binds to the acidic components of cytoplasm, especially to the RNA rich ribosomes, nuclei and nucleoli (Figure 7). The protocol is short, where all solutions have high alcohol concentration. It has previously been reported that ethanol based staining, together with short time, improve the integrity of RNA. Still the staining may possibly interfere with RNA extraction, thus, affecting the RNA degradation during the process of staining [90, 91].

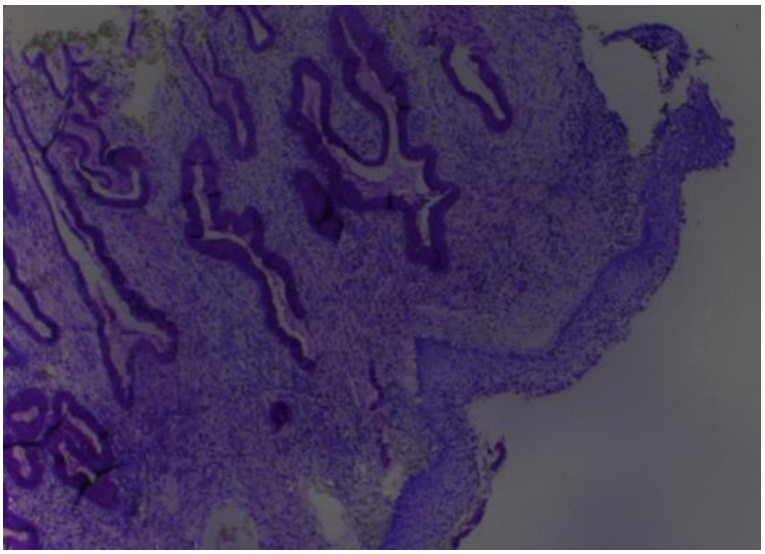

Figure 7. Cervical tissue stained with cresyl violet.

1.5 Laser microdissection

Laser MicroDissection (LMD) tools are designed to selectively and precisely isolate cell populations from tissues of interest [92]. LMD can be performed on a number of tissues, and tissues treated in different ways, such as FFPE- and fresh frozen tissues. When identifying

areas of interest by morphology and immunohistochemistry, staining with a histologic dye like cresyl violet makes the visualization easier. The tissue section is first placed on a membrane slide. The membrane slide is inert and will not affect further analysis of the sample. The section on the membrane slide is protected by a glass slide to avoid contamination, and to protect the tissue from excess heat. LMD of a desired section is then performed by using a precisely focused UV-laser beam under a light microscope (Figure 8) [93]. LMD is a very accurate method, however, the amount of material obtained is small. In addition, the use of histologic dyes and the laser beam itself may affect the RNA quality of the samples [90].

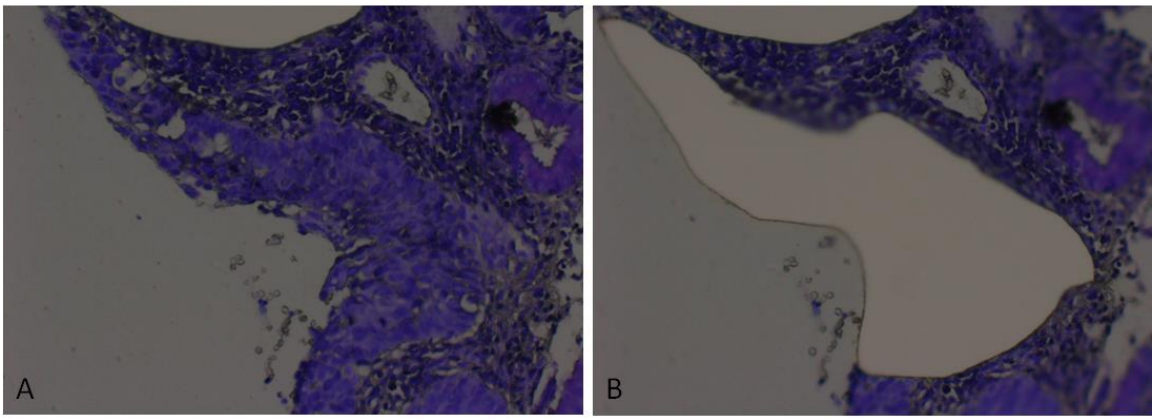

Figure 8. Picture A shows CIN3 tissue prior to laser microdissection, while picture B shows the same tissue after epithelium are removed by laser microdissection.

1.6 RNA extraction

The importance of RNA analysis has increased the past decades, thus, established a growing demand for commercially available kits, designed to purify high quality RNA [94]. Obtaining high-quality RNA is the first and often the most critical step in performing a multitude of molecular techniques including RT-PCR, microarrays, RNA mapping and northern blot analysis [95].

Three common approaches are used for extraction of RNA:

1. Organic extraction method: The sample is homogenized in a phenol-containing solution, and centrifuged. During centrifugation the sample is separated into three

phases, a lower organic phase, a middle protein and DNA containing phase and an upper RNA containing phase. The RNA containing phase is recovered and treated with alcohol precipitation and rehydration.

2. Membrane based method: Nucleic acid binds to a membrane fleece (usually glass fiber), in the presence of a chaotropic salt, usually guanidine. The RNA is lysed in the chaotropic salt containing RNase inhibitors and bound to the membrane by using centrifugal force. Series of rapid wash-and-spin steps are used to remove contaminants, and the RNA is eluted in a last step using a low-salt solution such as RNase free water.

3. Magnetic particle method: Particles with paramagnetic core is modified to bind to molecules of interest when exposed to a magnetic field. Once the field is removed the molecules are easily resuspended in a solution containing RNase inhibitor, and collected by applying a magnetic field. After several rounds of resuspension and collection in wash solutions, the RNA is released by elution buffer and the particles are removed.

Many purification protocols often have common requirements. When using archival tissue, such as FFPE tissue, a deparaffinization method is needed prior to the RNA extraction. Then, proteinase K is used to release RNA molecules from the sections. In order to improve the RNA quality, a short incubation time at higher temperatures are conducted to partially reverse crosslinking of the released nucleic acids [94].

1.7 Nanodrop

A wide range of biomolecules absorb light at characteristics wavelengths, this light absorption can be measured by a spectrophotometer. By measuring the light intensity of a reference solution and a sample solution at a given wavelength, the sample intensity compared to reference intensity is used to calculate the sample absorbance by the Beer-lambert equation:

$$log = \frac{Io}{I} = \varepsilon cl$$

$$A = -log = \frac{I}{Io}$$

A is the absorbance (also called the optical density), I_o is the intensity of the incident light, *I* is the intensity of the transmitted light, ε is the molar absorptivity coefficient (units of liter/mol–cm), *l* is the pathlenght in cm and *c* is the concentration of the absorbing specie in moles/liter [96].

For nucleic acid calculation, the Beer-lambert equation is modified:

$$c = \frac{(A \cdot \varepsilon)}{l}$$

A is the absorbance, *c* is the nucleic acid concentration in ng/microliter, ε is the molar absorptivity coefficient (units of microliter/ng–cm), *l* is the pathlenght in cm [97].

RNA purity can be measured photometrically with of a spectrophotometer such as NanoDrop™ (Thermo Fisher Scientific). The optical density is measured at different wavelengths; 280nm (absorption maxima of proteins), 260nm (absorption maxima of nucleic acids) and 230nm (absorption of contaminants and background absorption) [98]. The ratio of $OD_{260/280}$ ≥1.80 indicates satisfactory purity of isolated RNA. Lower values indicates presence of contaminants, but may still function well for quantitative PCR or other downstream applications [94]. The $OD_{260/230}$ ratio is a secondary measure of nucleic acid purity and the value is often higher than for $OD_{260/280}$, commonly 1.80-2.20. Lower ratio may indicate presence of copurified contaminants [97].

1.8 Bioanalyzer

Due to the instability of RNA and the environmental presence of RNases, integrity measurements are important prior to an RNA-dependent analysis [99]. RNA degradation can be measured by electrophoretic methods. Traditionally, gel electrophoresis stained with ethidium bromide has been used. To determine high quality RNA, bands consisting of 28S and 18S ribosomal RNA species are located. If the 28S:18S bands are about 2.0 and higher the RNA is considered high quality. This technology is somewhat time-consuming, relies on human interpretation and may be hard to compare from one laboratory to another [100].

In 1999, Agilent Technologies introduced the Bioanalyzer 2100, an automated lab-on-chip device that use capillary electrophoresis for the analysis of RNA integrity. The device generates an electropherogram and a gel image, and the 28S / 18S ratio can be calculated by looking at the peaks of the electropherogram and the bands of the gel [98, 100]. Different types of chips are available, depending on what type of RNA is of interest to measure. The Agilent Small RNA kit (Agilent Technologies) makes it possible to analyze small RNA nucleotides (nt) in a sample (Figure 9). The kit defines miRNA as RNA fragments within a size of 15–40 nt, but most scientist agree that miRNA is defined within the length of 19-25 nt [80, 101, 102]. Degradation of longer RNAs can lead to formation of small RNA within the range of 15 -40nt, and is therefore important to take into account, when analyzing results from FFPE samples [98].

Figure 9. Bioanalyzer 2100 with Small RNA chip [103].

1.9 Real time quantitative PCR (RT-qPCR)

Polymerase chain reaction (PCR) is a biotechnical method used for amplification of one specific DNA sequence into millions of molecules with identical sequences and making detection possible. This process was invented by Kary Mullis in 1983, and became so popular and indispensable in medical and biological research, that Mullis was rewarded the Nobel Prize in chemistry in 1993 [49]. Essential steps for PCR, when the starting material is RNA, are shown in Figure 10.

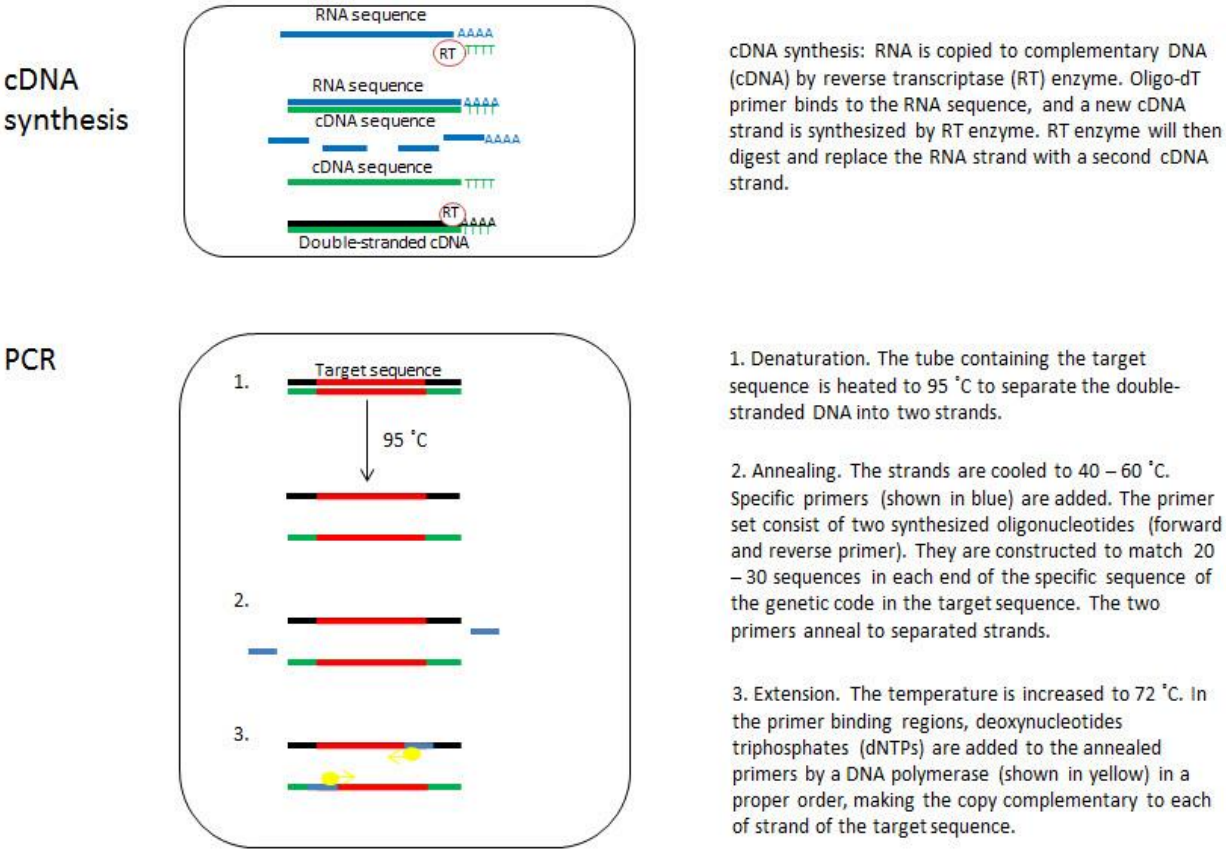

Figure 10 show an overview of cDNA synthesis and PCR.

Negative and positive controls are essential during PCR analysis. A “negative control” consists of the PCR mixture, but the template is substituted by water. A “positive control” is typically a good-quality DNA template, amplified with the same primers as the sequence of interest. The control sample is a good indicator of whether or not any of the PCR components have failed during the PCR protocol steps [104].

Primers are short DNA sequences (18-24nt) designed to recognize the sequence of interest [105]. A primer-pair is designed to recognize each end of a specific DNA/mRNA or miRNA sequence of the target tissue. The primer-pair consist of two nucleotide sequences. One sequence targets the 5`- 3` direction end of the template and is called “forward primer”. The other sequence targets the 3`- 5` direction and is called the “reverse primer”. Different aspects are important when choosing a primer:

- The size of the template depends of the distance between the binding sites of the forward and reverse primer. If the template size is too big, higher temperature and longer time is needed for the PCR process to be fulfilled.

- The percentages of guanine and cytosine should not exceed 50–60 %. Guanine and cytosine requires more thermal energy to brake because they possess three hydrogen bonds, while adenine and thymine only possess two. For primers shorter than 20 bases, T_m can be calculated by using the following formula; $T_m = 4(G+C) + 2(A+T)$ [105].

- The melting temperature of the primer should be similar to the T_m of the template.

- Primers should not be complementary to each other, and is particular important regarding their 3'-ends. Complementarity may lead to primer-dimer, in which the PCR product is a result of the amplification of the primers themselves [106].

When the starting material is RNA, reverse transcriptase is the first step for real time quantitative PCR (RT-qPCR). Reverse transcriptase is an enzyme used to convert RNA to complementary DNA (cDNA) prior to the qPCR reaction. RNA is either reverse transcribed using specific primers or RNA molecules are tailed with a common sequence and then transcribed using a universal primer (Figure 10) [107]. It is important to add a "negative control" during the synthesis of cDNA. In a "negative control" the reaction enzyme is not added to the cDNA mixture, thus, there should be no DNA products to be amplified in the PCR reaction [104].

Real time PCR is identical to conventional PCR, except that amplification of a target sequence emits a fluorescent signal that can be measured in the cycle-to-cycle progress of the reaction. Hence, the number of copies increased is measured real time by increased fluorescence during reaction. Because the amplified product is measured real time, there is no need for analysis on an agarose gel after the PCR reaction has finished. The reaction is run, and data evaluated in a closed environment reducing the contamination opportunity and eliminating the need for post-amplification manipulation [106, 108]. Three phases defines the process of real time PCR; the exponential phase, the linear phase and the plateau region [109]. During the exponential phase, the production of new PCR products

doubles in each cycle. A linear phase follows the exponential phase as one or more of the components consumed becomes limiting. The efficiency slows down, and the increase will become more arithmetic, than exponential. The linear phase is not precise from sample to sample, due to dNTPs or primers are consumed at slightly different rates between reactions [109]. As the reaction slows down, it enters the plateau region. The components have reached the end of their effectiveness and the fluorescent signals levels out [110]. The first fluorescent signal is detected when there is a certain amount of amplified products and before the reagents become limited in the exponential phase. The cycle number at which this occurs is called the quantification cycle (C_q) according to the MIQE guidelines, Cq value may also be referred to as crossing point (C_p) or threshold (C_t) value in different literature [111]. The Cq value is determined by the amount of template at the start of the PCR reaction. When the amount of starting template is high and of good quality, only a few amplification cycles are needed to reach the threshold line. However, if the amount of starting template is low or of bad quality, more amplification cycles are required to reach the threshold line [106, 110].

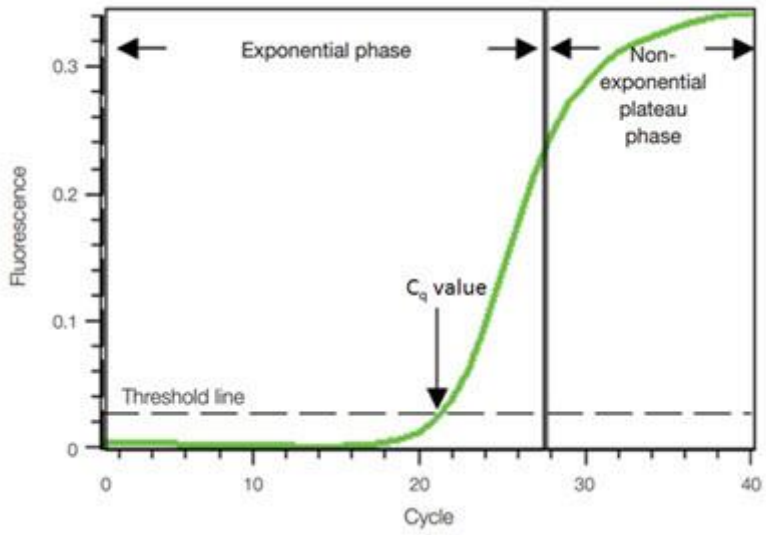

Figure 11 Amplification curve. PCR cycle numbers are shown on the x-axis and fluorescence from the amplification reaction is shown on the y-axis. Modified from [106].

The accuracy of a RT-qPCR analysis requires a proper standardization and normalization. The purpose of using standard reference genes for normalization is to increase the reliability and reproducibility of an experiment [112]. Due to their small sizes and tissue-specificity miRNAs

represents a significant challenge for normalization. The reference genes should have similar purification properties as the target miRNA, and most importantly, expression of a reference gene should not differ between normal and tumor tissue of interest [55].

SYBR green is a simple and cheap intercalating fluorescent dye used in RT-PCR. SYBR green will only expose fluorescence signals when bound to the double-stranded DNA, thus, during amplification increased amounts of dye binds to dsDNA as they are generated. A disadvantage of SYBR green is that it cannot discriminate between different PCR products and will bind to all double-stranded DNA including primer-dimer [112]. After the amplification reaction is completed, a melting curve is generated by increasing the temperature. When the temperature reach a certain melting peak, the dsDNA "melts" into single-strand DNA, and the fluorescent signal decreases. All PCR products in the reaction should have a single peak in the melting curve, whilst occurrence of multiple peaks on a melting curve indicates the presence of nonspecific products.

1.10 Chromogenic *in situ* hybridization (CISH)

In situ hybridization (ISH) is a common method for visualizing nucleic acid targets within fixed tissue and cell types, and is based on a method where a DNA/RNA probe joined with a marker can hybridize on a specific target. The method is a time consuming and difficult process which requires protocol optimizing to achieve satisfactory ISH results [113].

Small RNA such as miRNA makes ISH a challenging technology [114]. Before a probe is hybridized into the fixed tissue, the visibility of the nucleotide sequence has to be increased while still maintaining the structural integrity of the tissue. This can be done by using a protease to digest the tissue over a fixed length of time. Hybridization is done with a suitable probe. When working with miRNA, a diluted Locked Nucleic Acid (LNA™) oligonucleotide probe (Exiqon) is preferred due to the short length and fragile nature of these RNA molecules [115]. Nucleosides are a class of nucleic acid analogues where a methylene bridge is formed on the ribose backbone connecting the 2'-O atom and 4'-atom (in a three-dimensional space), which locks the nucleotide into place after hybridization (Figure 12). This complex increases the melting temperature, thus, makes it more difficult for the LNA probe and the complementary miRNA sequence to degrade [116]. Hybridization temperature is a

critical parameter in the protocol, and it is advisable to use the highest possible hybridization temperature to avoid cross hybridization with similar complementary sequences [114].

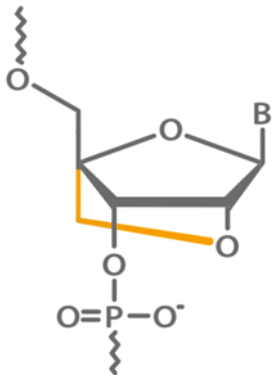

Figure 12. Locked Nucleic Acid (LNA) nucleoside [117].

Chromogenic *In Situ* Hybridization (CISH), uses a mix of hybridization and immunohistochemistry techniques where the probe-target complex is targeted with antibodies. This makes the complex visible in a light microscope. In the mirCURY LNA™ miRNAISH optimization kit (Exiqon), non-mammalian hapten digoxigenin (DIG) is labeled to the LNA probes. DIG is then recognized by specific antibodies conjugated the enzyme Alkaline Phosphatase (AP), which converts 4-nitro-blue tetrazolium (NBT) and 5-bromo-4-chloro-3'-indolylphophate (BCIP) into dark-blue NBT-BCIP substrate and water (Figure 13). A nuclear counterstain such as nuclear fast red is used to stain the nuclei pale pink for better histological resolution [113, 116].

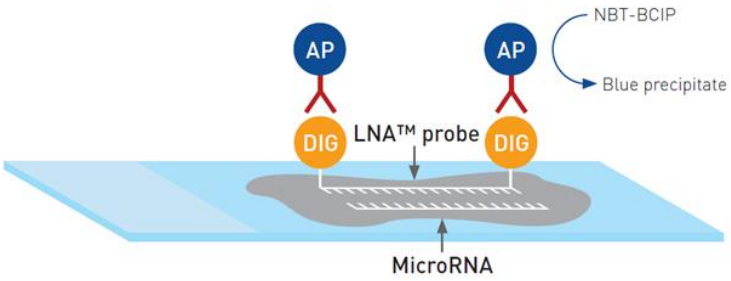

Figure 13. Illustration of Chromogenic in situ hybridization using the mirCURY LNA™ miRNAISH optimization kit from Exiqon [113].

2 Aim of the thesis

The aim of this thesis was to optimize methods for isolation, purification and detection of miR-18a and miR-18b in FFPE cervical specimens. We wanted to test two kits, miRNeasy FFPE kit from Qiagen and High Pure FFPET RNA isolation kit from Roche Diagnostics, for extraction of RNA. Epithelial and stromal cells were separated with microdissection and whole sections were macrodissected. We wanted to compare the expression of miR-18a and -18b in persistent HPV-16 positive CIN3 samples and normal cervical samples by the use of RT-qPCR and semi-quantitative scoring with CISH.

3 Material and methods

3.1 Patient samples

In a prospective study, women age 25–40 with detected atypical cytological smears were referred to the gynecology outpatient clinic at Stavanger University Hospital between January 2007 and December 2008. In total 254 patients were referred for a cervical punch biopsy and 170 had a high grade CIN (CIN2-3) and were treated with conization. They had follow-up of at least 3 visits to the gynecology outpatient clinic. Conization material and punch biopsies were fixed in 4 % buffered formaldehyde for 24–48 hours at 20 ˚C and embedded in paraffin at 56 ˚C. Sections from FFPE biopsies were used in this thesis. The sections were analyzed by two experienced histopathologists (Figure 16). The pathologist identified and marked the areas of target tissue by additional use of ki67 and p16 expression, which met the requirements of the study (CIN3).

In total 60 patient samples were excluded due to; pregnancy, previous treatment of CIN and biopsy cone excision interval shorter than 80 days, disease or treatment affecting the immune system, insufficient material for immunostaining and negative linear array in HPV genotyping test.

Of the remaining patients, HPV genotype 16 was found in 32 patients and HPV genotype 16 + other high-risk HPV in 22 patients. Regression was defined as a CIN2-3 diagnosis in the cervical biopsy and CIN1 or less in the cone. 37 patients had normal biopsies, considered as ki67 normal and p16 negative. For this study we chose to do experiments on 20 persistent HPV-16 positive CIN3 biopsies, and compare them to 20 normal biopsies.

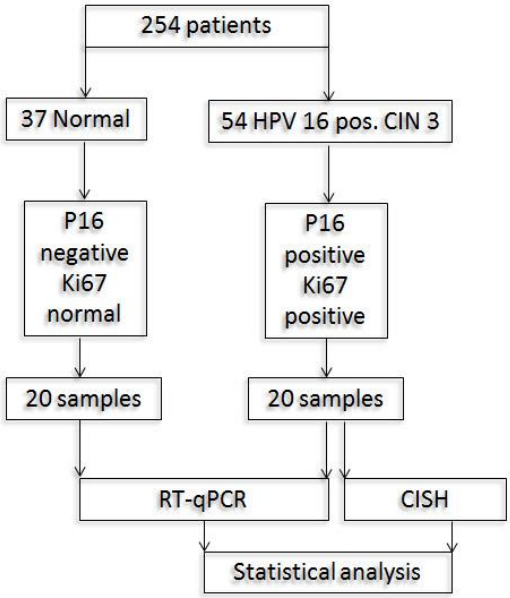

Figure 14. Expression of miR-18a and miR-18b in 20 normal cervical samples and 20 persistent HPV-16 pos. CIN3 samples were investigated. qPCR was used to compare expression of the miRNAs, while CISH was used for visualization.

3.2 General considerations and requirements

To ensure a DNA and RNA free working area, some general consideration were followed:

- All work was performed in a fume hood, if nothing else is stated.
- All working areas and equipment were treated with UV-light, chloride, ethanol and / or RNase zap prior to use.
- RNase free gloves were worn at all times, and changed frequently.
- Glassware equipment was washed and autoclaved if possible.
- MQ water was always used, if nothing else is stated.
- All solutions used were sealed in an RNase free container at all times.

- Microtome used for sectioning FFPE blocks was thoroughly washed with RNA wipes and nuclease free water prior to use.

3.3 Cresyl Violet staining for laser microdissection

Two sections (5µ) from the biopsies were cut on a microtome and mounted on a membrane slide. An additional section for H&E staining was cut as a control to ensure that the lesion was still present in the tissue block. The sections were kept in a fridge overnight and colored with cresyl violet staining the following day.

Reagents and equipment used in this experiment are listed in Table 2. Suppliers are listed in appendix 9.1.

Table 2. Reagents and equipment used during this experiment.

Reagents	**Equipment**
Xylene	MMI membrane slides embedded with FFPE tissue
99.9 % ethanol	Tweezers
96 % ethanol	9x Containers (must be able to contain glass slides)
70 % ethanol	Pipet-lite
50 % ethanol	Paper towels
Cresyl violet	Weight
MQ water	Weighing boat
Acetic acid	Measuring cylinders
	Slide rack
	Barrier pen (Dako)
	50 ml tubes

The cresyl violet solution:

250 mg cresyl violet was mixed with 39.25 ml MQ H_2O in a tube, then 10 ml ethanol (99.9 %) and 0.75 ml acetic acid (100 %) was added. The solution is stable in approximately 1 year.

Protocol:

1. The tissue sections were deparaffinized in xylene at 3 x 5 minutes (change container to new xylene after 5 minutes, 3 times).
2. The sections were rinsed in 99.9 % ethanol for 5 minutes. The ethanol was changed once within the 5 minutes.
3. The sections were rinsed in 96 % ethanol for 5 minutes. The ethanol was changed once within the 5 minutes.
4. The sections were rinsed in 70 % ethanol for 5 minutes. The ethanol was changed once within the 5 minutes.

The sections were dried horizontally on a slide rack until the excess ethanol had evaporated. The area to be colored with cresyl violet was marked with a Barrier Pen and 300 µl cresyl violet solution was added directly to the sections. After 20 seconds (sec) incubation, the sections were dried horizontally on a slide rack. The sections were dehydrated as followed:

1. Sections were rinsed in 50 % ethanol for 25-30 sec. The ethanol was changed once within those seconds.
2. Sections were rinsed in 70 % ethanol for 25-30 sec. The ethanol was changed once within those seconds.
3. Sections were rinsed in 96 % ethanol for 30-40 sec. The ethanol was changed once within those seconds.
4. Sections were rinsed in 99.9 % ethanol for 30-40 sec. The ethanol was changed once within those seconds.

The slides were stored at –80 ˚C prior to dissection.

3.4 Laser microdissection

During this experiment, macrodissected samples mounted on membrane slides and colored with cresyl staining were used. MMI CellCut Plus laser with associated software program (Molecular Machines & Industries) was used to cut and separate epithelium and stroma.

Reagents and equipment used in this experiment are listed in Table 3. Suppliers are listed in appendix 9.1.

Table 3. Reagents and equipment used during this experiment.

Reagents	**Equipment**
PKD Buffer from miRNeasy kit (Qiagen)	Microscope
Lysis Buffer from High Pure FFPET RNA isolation kit (Roche)	MMI CellCut Plus laser
	Isolation tube with diffuser cap and adhesive lids, 0.5 ml
	Membrane slides with 1.4 µm PET membrane
	Pipettes with corresponding pipette tips.

1. The microscope and MMI CellCut Plus laser were switched on and the associated software program was started.
2. The membrane slide with tissue section was placed on the microscope platform with a glass slide underneath.
3. The slide was scanned in order to make an overview of the section.
4. MMI isolation tube with adhesive cap was placed onto a holder and attached to the microscope.
5. The area of interest was marked and cut loose by the laser beam.
6. The loose tissue piece with the PET membrane was collected by adhesive forces in the cap as the holder was moved to a downward position.
7. Epithelium and stroma were cut separately. When desirable amount of tissue was collected, the cap holder was loosened from the microscope.

8. Either 150 µl PKD buffer or 100 µl lysis buffer was added to the isolation cap.
9. After incubation for 10 minutes, the sample was spun down briefly and kept at – 80 ˚C until RNA extraction was performed.

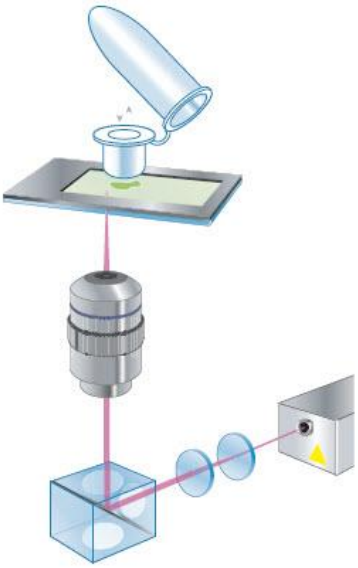

Figure 15. The principle of microdissection with MMI CellCut Plus Laser [93].

3.5 Macrodissection

Histological sections identified and marked by a pathologist were used in this study (Figure 16). Whole sections from the marked areas (5 µm) were precisely cut out with a microtome, and used in further analysis. One section was mounted on a slide for CISH analysis. Two sections were transferred to an Eppendorf tube for RNA extraction and the last section was mounted on a slide for H&E staining as a control to ensure that the lesion was still present in the tissue block.

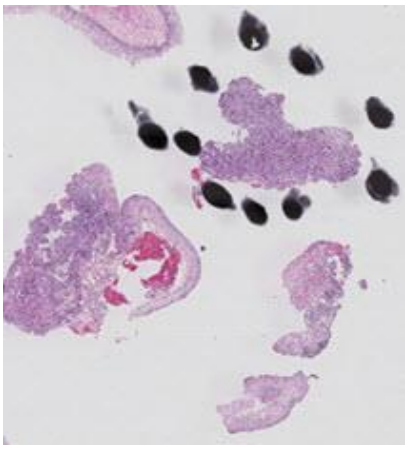

Figure 16. The area of interest within a histologic section is analyzed and marked by a pathologist.

3.6 RNA extraction

3.6.1 High Pure FFPET RNA isolation kit

RNA from laser microdissected samples were extracted using High Pure FFPET RNA isolation kit from Roche Diagnostics.

Reagents and equipment used in this experiment are listed in Table 4. Suppliers are listed in appendix 9.1.

Table 4 Reagents and equipment used in RNA extraction with High Pure FFPET RNA isolation kit.

Reagents (in the kit)	**Equipment (in the kit)**
RNA Tissue Lysis Buffer	High Pure Filter Tubes
Proteinase K	Collection Tubes
RNA binding Buffer	Micro Tubes 1.5 ml
Sodium dodecyl sulphate	**Equipment (additional)**
Wash Buffer I	Centrifuge
Wash Buffer II	Pipette with corresponding pipette tips
DNase I	Vortex
DNase Incubation Buffer (1x)	Heating block with shaker
RNA Elution Buffer	50 ml test tubes
Reagent Preparation Buffer	

The following solutions were prepared prior to the experiment:

10 % sodium dodecyl sulphate:

5 g SDS was dissolved in 45 ml MQ water and kept in a 50 ml test tube at room temperature.

Proteinase K:

A fixed amount of proteinase K was dissolved in 4.5 ml Reagent Preparation Buffer. Aliquots were prepared and stored at –20 ˚C.

Wash Buffer I:

15 ml of 99.9 % ethanol was added to a fixed solution of Wash Buffer I and stored at room temperature.

Wash Buffer II:

80 ml of 99.9 % ethanol was added to a fixed solution of Wash Buffer II and stored at room temperature.

DNase I:

A fixed amount of DNase I was dissolved in 740 µl Reagent Preparation Buffer. Aliquots were prepared and stored at –20 ˚C.

The following solution was made during the experiment:

DNase working solution:

DNase working solution was prepared by using the equation below:

Required amount for number of (N) RNA isolations

((N + 1) x 90 µl DNase Incubation Buffer) + ((N + 1) x 10 µl DNase I)

Protocol:

1. 16 µl 10 % SDS and 40 µl Proteinase K was added to 100 µl RNA Tissue Lysis Buffer (containing microdissected tissue). The solution was vortexed for several seconds,

spun down briefly and incubated at 85 ˚C with shaking at 600 *rpm*. The solution was cooled to less than 55 ˚C and spun down.

2. 80 µl Proteinase K was added and the solution was vortexed, spun down and incubated at 55 ˚C with shaking at 600 *rpm*. The solution was spun down briefly. The lysate should now be clear, if not, the incubation can be extended for 10 minutes.
3. 325 µl RNA Binding Buffer and 325 µl 99.9 % ethanol was added to the solution, vortexed and spun down.
4. High Pure Filter Tube was placed onto High Pure Collection Tube. The lysate was pipetted into the upper reservoir of the filter tube and centrifuged for 30 seconds at 6000 *x g*.
5. The High Pure Filter Tube was placed onto a new High Pure Collection Tube and centrifuged for 2 minutes at 16 000 *xg*.
6. The High Pure Filter Tube was placed onto a new High Pure Collection Tube. 100 µl DNase working solution was pipetted onto the fleece of the filter tube (without touching the fleece) and incubated at 15 minutes in room temperature.
7. 500 µl Wash Buffer I working solution was added to the filter tube and centrifuged for 20 seconds at 6000 *x g*. The flow through was discarded.
8. 500 µl Wash Buffer II working solution was added to the filter tube and centrifuged for 20 seconds at 6000 *x g*. The flow through was discarded.
9. 500 µl Wash Buffer II working solution was added to the filter tube and centrifuged for 20 seconds at 6000 *x g*. The flow through was discarded. The tube was then centrifuged for 2 minutes at 16 000 *x g* to dry the filter fleece. The High Pure Filter Tube was then placed into a new 1.5 ml reaction tube.
10. 25 µl RNA elution buffer was pipetted onto the fleece of the filter tube (without touching the fleece) and incubated at 1 minute in room temperature. The tube was then centrifuged for 1 minute at 6000 *x g*.

The eluted RNA samples were stored at –80 ˚C.

3.6.2 miRNeasy FFPE kit

RNA was extracted using miRNeasy FFPE kit from Qiagen. RNA extraction was either performed on laser microdissected tissue, or macrodissected tissue. An additional deparaffinization step was added prior to extraction of RNA from macrodissected tissue.

Reagents and equipment used in this experiment are listed in Table 5. Suppliers are listed in appendix 9.1.

Table 5. Reagents and equipment used in RNA extraction with miRNeasy FFPE kit protocol.

Reagents (in the kit)	**Equipment (in the kit)**
PKD Lysis Buffer	Spin Columns in 2.0 ml collection tubes
Proteinase K	2.0 ml collection tubes
DNase I	1.5 ml collection tube
DNase Booster Buffer	**Equipment (additional)**
Buffer RBC	Micro Tubes 1.5 ml
Buffer RPE	Pipette with corresponding pipette tips
RNase-free water	Vortex
Reagents (additional)	Centrifuge
Xylene	Heating block with shaker
99.9 % ethanol	50 ml test tubes

<u>The following solutions were prepared prior to the experiment:</u>

<u>DNase I:</u>

Lyophilized DNase I was dissolved in 550 µl MQ-water. Aliquots were prepared and stored at –20 ˚C.

<u>RPE Buffer:</u>

44 ml of 99.9 % ethanol was added to a fixed solution of RPE buffer and stored at room temperature.

Protocol:

Deparaffinization of FFPE tissue:

1. 1 ml xylene was added to the FFPE tissue. The solution was vortexed for 10 seconds and centrifuged at full speed for 2 minutes.
2. The supernatant was carefully removed, and 99.9 % ethanol was added.
3. The solution was vortexed for 10 seconds and centrifuged at full speed for 2 minutes.
4. The supernatant was carefully removed and the tissue was incubated at 37 ˚C until all residual ethanol had evaporated.

RNA extraction:

1. 150 µl PKD buffer was added to the sample and mixed by vortexing.
2. 10 µl Proteinase K was added and mixed gently by pipetting.
3. The solution was incubated for 15 minutes at 56 ˚C with shaking at 600 *rpm*, then at 80 ˚C for 15 additional minutes.
4. The lower clear phase was transferred into a 2.0 ml microcentrifuge tube, incubated on ice for 3 minutes and centrifuged for 15 minutes at 20 000 *x g.*
5. The supernatant was transferred to a new 2.0 ml microcentrifuge tube.
6. 16 µl DNase booster buffer and 10 µl DNase was added to the tube, mixed by pipetting, and centrifuged briefly.
7. The solution was incubated for 15 minutes at room temperature.
8. 320 µl RBC buffer was added to the tube and mixed thoroughly.
9. 1120 µl 99.9 % ethanol was added to the solution and mixed by pipetting.
10. 700 µl of the sample was added to an RNeasy MinElute spin column placed in a 2.0 ml collection tube. The spin column was centrifuged for 15 seconds at ≥ 8000 *x g.* Flow-through was discarded.
11. Step 10 was repeated until the entire amount of sample had passed through the spin column.
12. 500 µl Buffer RPE was added to the spin column and centrifuged for 15 seconds at ≥ 8000 *x g*. Flow-through was discarded.

13. 500 µl Buffer RPE was added to the spin column and centrifuged for 2 minutes at ≥ 8000 *x g.* Flow-through was discarded along with the collection tube.
14. The spin column was placed in a new 2.0 ml collection tube, the lid kept open, and centrifuged at full speed for 5 minutes. Flow-through was discarded along with the collection tube.
15. The spin column was placed in a new 1.5 ml collection tube. 12 µl MQ water was added directly on the membrane without touching the fleece, and centrifuged for 1 minute at full speed.
16. Step 15 was repeated.

The eluted RNA samples were stored at –80 °C.

Some modifications of the miRNeasy protocol were made during the thesis to optimize the purity of RNA:

- Step 3: The 15 minutes incubation incubated for 15 minutes at 56 ˚C with shaking at 600 *rpm*, was increased to 1 hour.
- Step 12 was repeated, with one extra round with washing buffer.
- Step 15- 16: 12 µl MQ water was added directly on the membrane without touching the fleece, incubated for 10 minutes and centrifuged for 1 minute at full speed. 12 µl MQ water was added once again, without incubation time, but directly centrifuged for 1 minute at full speed.

3.7 Nanodrop 2000

Concentration of the newly extracted RNA was measured by Nanodrop 2000 UV-Vis Spectrophotometer (Thermo Scientific).

Reagents and equipment used in this experiment are listed in Table 6. Suppliers are listed in appendix 9.1.

Table 6. Reagents and equipment used during the experiment.

Reagents	**Equipment**
MQ water	Spectrophotometer
	Pipette with corresponding pipette tips
	Vortex

The samples were vortexed, spun down and kept on ice during the measurements.

Protocol:

1. Nanodrop program with application “Nucleic acid” was chosen. The type was set to “RNA” and the concentration set to ng/µl.
2. A blank was measured using 1.5 µl MQ water.
3. Between each measurement the reagent was wiped off the pedestal of the instrument with a clean paper towel.
4. 1.5 µl of samples were measured. The reagents were wiped of the pedestal with a clean paper towel before each new measurement.
5. After measurements the NanoDrop was cleaned with 5 µl MQ water for 2 minutes.

The samples were stored at –80 ˚C.

3.8 Agilent 2100 Bioanalyzer

Concentration of the newly extracted RNA was measured by Agilent 2100 Bioanalyzer (Agilent Technologies), by the use of Small RNA kit (Agilent Technologies).

Reagents and equipment used in this experiment are listed in Table 7. Suppliers are listed in appendix 9.1.

Table 7. Reagents and equipment used during the experiment.

Reagents (in the kit)	**Equipment (in the kit)**
Dye concentrate	RNA chip
RNA Marker	**Equipment (additional)**
RNA Conditioning Solution	PCR strip tubes with associated caps.
RNA Gel Matrix	Heating block
RNA Ladder	Agilent 2100 Bioanalyzer
RNase free water	Vortex
RNaseZAP	Microcentrifuge
	Syringe
	Spin filter columns
	Pipette with corresponding pipette tips
	0.5 ml microtube

The following solutions were made prior to the experiment:

RNA samples:

The total amount of purified small RNA in sample should be between 1–20 ng/µl. If a sample was above this range, dilution with MQ-water was performed. The diluted RNA samples were denatured for 2 minutes at 70 ˚C and immediately cooled down prior to use.

RNA Ladder:

The ladder was denatured for 2 minutes at 70 ˚C and immediately cooled down on ice. Aliquots were prepared in 0.5 ml microtubes. The ladder was stored at –80 ˚C.

Gel matrix:

The complete volume of the gel matrix (650 µl) was pipetted into a spin filter column. The spin filter was centrifuged at 10 000 *x g* for 15 minutes. The gel could be stored up to a month.

The samples were kept on ice and reagents in room temperature during the experiment.

Protocol:

Loading the Gel-Dye mix:

1. A new RNA chip was put on the chip priming station.
2. 9 µl of Gel-Dye mix was loaded in a specifically marked well.
3. The chip priming station was closed and the plunger of the syringe was set at 1.0 ml. The plunger was pressed down until it was held by a clip.
4. After 60 seconds, the clip was released and the plunger moved back to 0.7 ml mark.
5. After 5 seconds, the plunger was pulled back to 1.0 ml mark, and the chip was removed.
6. 9 µl of Gel-Dye mix was loaded in two specifically marked wells.

Loading the Condition solution and Marker:

1. 9 µl of the RNA conditioning solution was pipetted into the well named CS.
2. 5 µl of RNA marker was pipetted into all sample wells, including the well for the ladder.

Loading the Ladder and Samples:

1. 1 µl of ladder was loaded in the well for the ladder.
2. 1 µl of sample was loaded in the sample wells.
3. 1 µl of RNA marker green was added in unused wells.
4. The chip was run in the Agilent 2100 Bioanalyzer within 5 minutes.

The Bioanalyzer was cleaned with RNase-free water for 5 minutes.

3.9 RT-qPCR

The work was done in separate rooms, pre-PCR room and template room. DNA and RNA products are prohibited in the pre-PCR room. PCR products are prohibited in the template room. This is done to prevent contamination of solutions and material. All solutions were

made in pre-PCR room, and transferred to the template room, and added template. In addition to using separate rooms, two negative controls; no-Reverse transcriptase (noRT) and no-template-control (noTC) were used. noRT control is used to detect contamination in cDNA kit solutions, while noTC detects contamination in SYBR green master mix solutions. noRT and noTC should not amplify in the PCR reaction. MCF-7 (breast cancer cell line) was used as a positive control. In addition, spike-in control was used when analyzing microdissected samples, to test the sample tissue for the potential presence of PCR inhibitors.

Reagents and equipment used in this experiment are listed in Table 8. Suppliers are listed in appendix 9.1.

Table 8. Reagents and equipment used during the experiment.

Reagents (in the kit)	**Equipment (additional)**
Universal cDNA synthesis kit:	Pipette with associated pipette tips
5 x Reaction buffer	Vortex
Enzyme mix	Micro tubes 1.5 ml
Nuklease-free water	Heating block.
RNA spike-in control	8 strip PCR tubes (0.2 ml) with associated caps
	Sealing foil
	Light cycler 480 (Roche)
SYBR Green master mix, Universal RT, 2.5 ml:	
SYBR Green master mix	
Nuklease-free water	
Control primer set	
miRCURY LNA™ Universal RT miRNAPCR, reference-gene primer set (miR-23a, miR-191, miR-18a, miR-18b):	
LNA Forward Primer	

LNA Reverse Primer	

Following solutions were made prior to the experiment:

Spike-in:

RNA spike-in was dissolved in 40 µl (a second batch was dissolved in 80 µl) nuclease-free water, vortexed and spun down briefly. Aliquots were stored at -20 ˚C.

Primers:

Forward and reverse primer were dissolved in 110 µl nuclease free water, vortexed and spun down briefly. The primers were mixed by adding 110 µl forward primer in reverse primer, vortexed and spun down. Aliquots were stored at -20 ˚C.

Protocol:

Step 1: Synthesis of the cDNA template strand:

1. Pre-PCR lab: The reaction buffer, enzyme mix and nuclease free water were taken out from the freezer and put in a light protected box for thawing.
2. Template lab: The concentration of RNA template should optimally be 5 ng/µl. This is reached by adding water and a calculated amount of sample. The final amount of template should be 4 µl.
3. Pre-PCR lab: A fixed amount of reaction buffer and nuclease free water was added to a microtube after being vortexed and spun down briefly.
4. Pre-PCR lab: A fixed amount of enzyme mix was added to the microtube after being flicked and spun down briefly. Enzyme mix was replaced with water in the no-RT control mix.
5. Template lab: The cDNA master mix was transferred to the template room where 15 µl cDNA master mix and 1 µl RNA spike-in were added to each of the 0.2 ml tubes containing the template (5 ng/µl).
6. 4 µl of template (5 ng/µl) were added in the tube containing no-RT control mix.

7. Template lab: The samples were placed in ThermoStat plus at 42 ˚C for 1 hour and 95 ˚C for 5 minutes.

Step 2: Real time PCR amplification with different micro PCR primers:

1. Pre-PCR: Master mix reagents were taken out from the freezer and put in a light protected box for thawing.
2. Pre-PCR: The different PCR primer mixes were vortexed and spun down. The SYBR Green master mix was flicked 15–20 times and spun down briefly. A fixed amount of primer (including spike-in primers) was added to different microtubes, one tube for each primer. A fixed amount of SYBR Green master mix was then added to the different tubes.
3. Pre-PCR: 6 µl of the primer solutions were added to labeled wells of a 96 well plate. The primer mix was added in duplicates or triplicates. The well was sealed with sealing foil.
4. Template lab: cDNA was diluted 1/40 or 1/80.
5. Template lab: The 96 well plate was transferred to the template room, where a 4 µl of cDNA was added to the different wells. The 96 well plate was sealed with sealing foil.
6. The plate was spun down for 1 minute, and amplified in the Lightcycler 480 (Roche Diagnostics).

The following settings for the light cycler program were used:

Analyse step	Temperature	Time
Polymerase activation/denaturation	95 °C	10 min
Amplification (45 cycles)	95 °C 60 °C Ramp rate 1,6 °C/ sec	10 sec 1 min

3.10 CISH

Histologic sections (5 µm) were cut from FFPE patient material by the use of a microtome and mounted onto SuperFrost plus slides, one day prior to the experiment. The sections were kept in a heating cabinet at 55 °C overnight, in order to make the wax melt and tissue stick to the slide. miR-18a and -18b hybridization probes were used as target probes for visualization of the miRNA. LNA™ scrambled probe was used as negative control (= no staining) and LNA™ U6 snRNA probe as positive control (= overall nuclear staining).

Reagents and equipment used in this experiment are listed in Table 9. Suppliers are listed in appendix 9.1.

Table 9. Reagents and equipment used during the experiment.

Reagents	**Equipment**
LNA™ miRNAprobe, double-DIG labeled miR-18a	1 L glass bottles
LNA™ miRNAprobe, double-DIG labeled miR-18b	Weight
LNA™ U6 snRNA, double-DIG labeled probe	Weighing boats
LNA™ scrambled, double-DIG labeled probe	Slides, SuperFrost plus®
99.9 % ethanol	Tweezers
96 % ethanol	Containers (must be able to contain glass slides)
70 % ethanol	Pipette with associated pipette tips
50 % ethanol	Slide rack
PBS tablets	Vortex
0.5 M EDTA	Centrifuge
1M Tris-HCl (pH =7.4)	Heating cabinet
NaCl	Hybridizer
Proteinase K stock solution	50 ml test tubes
20x SSC	Fixogum
Tris-HCl	Histokitt

KCl	Cover slips 24x55mm
NaCl	Clinical digital stop watch
Blocking stock solution	Moisture strips
Sheep serum	Measuring cylinders
Anti-DIG AP	Opaque containers
Tween-20	Microtubes 1.5 ml , 2.0 ml
NBT/BCIP	Paper towels
Levamisol stock solution	
Xylene	
2x ISH buffer	
10x Maleic acid buffer	
MQ water	
Tap water	
Nuclear fast Red	

The following solutions were made prior to the experiment:

PBS:

800 ml MQ water was added in a 1 L bottle. 5 tablets of PBS were dissolved in the water, and the volume was adjusted to 1000 ml.

PBS-T:

1000 µl Tween-20 was added to a PBS solution.

Proteinase K buffer:

900 ml MQ water was added in a 1 L bottle. 5.0 ml 1M Tris-HCl (pH=7.4), 2.0 ml 0.5M EDTA and 0.2 ml NaCl was then added to the water. The volume was adjusted to 1000 ml with MQ water.

5 x SSC:

250 ml 20 x SSC was added to a 1 L bottle containing 750 ml MQ water.

1 x SSC:

50 ml 20 x SSC was added to a 1 L bottle containing 950 ml MQ water.

0.2 x SSC:

10 ml 20 x SSC was added to a 1 L bottle containing 990 ml MQ water.

KTBT (AP-stop solution):

900 ml MQ water was added in a 1 L bottle. 7.9 g Tris-HCl, 0.75 g KCl and 8.7 g NaCl was then added to the water. The volume was adjusted to 1000 ml.

Proteinase K stock solution:

8 µl aliquots from Proteinase K stock solution were added to microtubes and stored at –20 ˚C.

The following solutions were during the experiment:

Proteinase K solution:

Proteinase K solution is made right before use with a desired amount of 15 µg/ml. 10 ml Proteinase K buffer and 7.5 µl proteinase K stock solution was added to a 50 ml test tube and mixed well.

Hybridization mix:

2 x ISH buffer was diluted to 1 x ISH by adding 0.5 ml 2 x ISH buffer and 0.5 ml MQ water to a microtube. 25 µM of LNA probes were denaturized at 90 ˚C for 4 minutes. The denaturized LNA probe was then diluted with 1 x ISH buffer to desired concentration. In our case the desired concentration was 80 nm (see equation below). 55 µl aliquots were transferred to microtubes and stored at -20 °C.

C_1 = 25 µM = 25000 nM; C_2 = 80 nM; V_2 = 658 µl; V_1 = ?

$$C1V1 = C2V2 \rightarrow V1 = \frac{C2V2}{C1} = \frac{80\ nM\ x\ 658\ \mu l}{25000\ nM} = 2.1056$$

Blocking solution:

1.1 ml 10x Maleic Acid buffer, 1.25 ml 10x Blocking solution stock and 0.25 ml sheep serum were added to a 50 ml test tube containing 9.9 ml water and mixed well. The solution should not be exposed to light, thus, the test tube was wrapped in aluminum foil.

Sheep anti-DIG-AP:

5 µl anti-DIG AP was added to a 50 ml test tube containing 4 ml blocking solution. The solution should not be exposed to light, thus, the test tube was wrapped in aluminum foil.

AP-substrate:

20 µl levamisol stock solution and 1 tablet of NBT/BCIP were added to a 50 ml test tube containing 10 ml water (the tablet must be completely dissolved before adding levamisol). The solution should not be exposed to light, thus, the test tube was wrapped in aluminum foil.

Protocol:

- The FFPE tissue sections were deparaffinized in xylene for 3 x 5 minutes (change container to new xylene after 5 minutes, 3 times).

The tissue sections were then rehydrated in ethanol:

1. The sections were rinsed in 99.9 % ethanol for 5 minutes. The ethanol was changed two times within the 5 minutes.

2. The sections were rinsed in 96 % ethanol for 5 minutes. The ethanol was changed once within the 5 minutes.
3. The sections were rinsed in 70 % ethanol for 5 minutes. The ethanol was changed once within the 5 minutes.

- The sections were washed in PBS for 2–5 minutes. PBS was changed once during this period.
- Proteinase K was made. The sections were placed on a hybridizer and 800 µl proteinase K solution was added to each section. Hybridization process was conducted at 37 °C for 25 minutes.

- The sections were washed in PBS for 2–5 minutes. PBS was changed one time during this period.

The sections were then dehydrated in ethanol:

1. The sections were rinsed in 70 % ethanol for 1 minute. The ethanol was changed once within the 1 minute.
2. The sections were rinsed in 96 % ethanol for 1 minute. The ethanol was changed once within the 1 minute.
3. The sections were rinsed in 99.9 % ethanol for 1 minute. The ethanol was changed once within the 1 minute.
4. The sections were air-dried on paper towel for 15 minutes.

- Moisture strips (containing 70 % ethanol) were placed in the lid of the hybridizer and the temperature was changed to 55 ˚C. Aliquots of hybridization mix (LNA probes) were thawed and centrifuged briefly. 50 µl of hybridization mix was added to each section, quickly covered with sterile coverslips and sealed with fixogum to prevent drying. The sections were placed on the hybridizer. Hybridization process was conducted at 55 °C for 1 hour.
- Fixogum was removed from the glass slides, and the slides were placed in 5 x SSC for 1 minute. The coverslips were carefully removed by using a tweezer.

The sections were washed in stringent wash:

1. The sections were rinsed in 5 x SSC holding a temperature of 55 °C for 5 minutes.
2. The sections were rinsed in 1 x SSC holding a temperature of 55 °C for 5 minutes.
3. The sections were rinsed in 1 x SSC holding a temperature of 55 ˚C for 5 minutes.
4. The sections were rinsed in 0.2x SSC holding a temperature of 55 °C for 5 minutes.
5. The sections were rinsed in 0.2 x SSC at room temperature for 5 minutes.

- The sections were washed in PBS.
- 800 µl of blocking solution was added to each section in a humidifying chamber to avoid exposure of light. The sections were incubated in the humidifying chamber for 15 minutes. 4.0 ml of blocking solution was used to make Sheep anti-DIG-AP.

- The incubated blocking solutions were discarded and the sections transferred to the hybridizer and the temperature changed to 30 °C. 500 µl of Sheep anti-DIG-AP was added to the sections and incubated for 45 minutes.
- The sections were washed in PBS-T for 9 minutes whereas PBS-T was discarded and new PBS-T was added 3 times (3 x 3 minutes).
- The sections were transferred to the hybridizer and 400 µl of AP substrate was added to each section. The sections were incubated in the humidifying chamber at 30 °C for 110 minutes.
- The sections were incubated in KTBT buffer for 10 minutes. KTBT was changed after 5 minutes (2 x 5 minutes).
- The sections were washed with MQ water for 2 minutes. MQ water was changed one time during these two minutes.
- Nuclear fast red was shaken thoroughly and sections were incubated for 3 minutes.
- The sections were then carefully rinsed with tapwater for 5 minutes.

The sections were rehydrated in ethanol:

1. The sections were rinsed in 50 % ethanol for 3 minutes.
2. The sections were rinsed in 70 % ethanol for 3 minutes.
3. The sections were rinsed in 96 % ethanol for 3 minutes.
4. The sections were rinsed in 99.9 % ethanol for 3 minutes.

- Immediately after rehydration, a drop of histokitt glue was added to the tissue section and sealed with coverslip. Air bubbles were carefully removed.

The tissue sections were analyzed in a microscope the following day.

3.11 Statistical analyses

SPSS (SPSS, Illnois, USA) predictive analytics software was used for statistical analysis. T-tests were used to compare miR-18a and -18b expression in HPV-16 positive CIN3 tissue and normal cervical tissue. Independent t-test was used when comparing 20 CIN3 patient samples and 20 normal cervical samples. Paired samples t-test was used when comparing

CIN3 lesions and normal cervical area within the same biopsy. Probabilities of 0.05 were considered as statistically significant. Boxplot were used to show the distribution of samples.

4 Results

4.1 Optimization of methods for extraction of miRNA from microdissected tissue

An experienced pathologist identified and marked the areas of interest in histological sections from patients included in the study. The sections were stained with cresyl violet for better microscopically visualization. By the use of laser microdissection technology, epithelium (E) and stroma (S) cells within the marked area were separated by a UV-laser and used for extraction of RNA from the cells of interest. The RNA was further used for measuring expression of miRNAs with quantitative PCR. The endogenous reference genes miR-23a and miR-191 were used.

4.1.1 Comparison of two different RNA extraction kits

Total RNA from the laser microdissected areas of one patient sample were extracted with two different kits to see which yielded the most satisfactory RNA purity. RNA extraction was performed with High Pure FFPET RNA isolation kit from Roche and compared with miRNeasy FFPE kit from Qiagen. The concentration and purity of the extracted RNA was measured photometrically by the use of Nanodrop (Table 10).

Table 10. Purity of extracted RNA when comparing High Pure FFPET RNA isolation kit from Roche and miRNeasy FFPE kit from Qiagen

Photometrical measurements				
Extraction kit	**Tissue section**	**ng/µl**	**$OD_{260/280}$**	**$OD_{260/230}$**
High Pure FFPET RNA isolation kit (Roche)	Epithelium	11.8	1.61	0.57
	Stroma	12.5	1.60	0.62
miRNeasy FFPE kit (Qiagen)	Epithelium	5.40	1.75	0.54
	Stroma	4.40	1.57	0.31

The purity and concentration of the eluted RNA was low after extraction with both kits. High Pure FFPET RNA isolation kit from Roche yielded the highest amounts of RNA with a mean concentration of 11.8 and 12.5 ng/µl. As shown with $OD_{260/280}$ and $OD_{260/230}$, the purity of extracted RNA from both kits was rather low. A PCR analysis was performed to test the quality of the miRNA in the extracted samples (Table 11).

Table 11. The mean Cq value for miR-191 using template extracted with High Pure FFPET RNA isolation kit from Roche and miRNeasy FFPE kit from Qiagen

PCR analysis		
Extraction kit	**Tissue section**	**Cq miR-191**
High Pure FFPET RNA isolation kit (Roche)	Epthelium	35.58
	Stroma	34.65
miRNeasy FFPE kit (Qiagen)	Epithelium	30.20
	Stroma	32.21

The quality of miRNA was less sufficient for PCR as showed with higher Cq values. By comparing Cq values, miRNeasy FFPE kit showed the best result, thus we continued to extract RNA from laser microdissected tissue with miRNeasy FFPE kit.

4.1.2 Optimization of miRNeasy FFPE kit

Modifications of the standard protocol regarding incubation time for proteinase K for the miRNeasy FFPE kit were tested, to further improve RNA quality of microdissected tissue. For the standard protocol, seven patient samples were used. Microdissected samples from two patients were used in modified protocol with prolonged incubation for 1 hour (1h) at 56 ˚C and incubation overnight (O/N) at 56 ˚C. The RNA concentration and purity were measured photometrically by the use of Nanodrop (Table 12).

Table 12 . The mean results of modifications to improve quality and yield of extracted RNA with miRNeasy FFPE kit from Qiagen

Photometrical measurements				
Extraction kit	**Tissue section**	**Mean ng/µl**	**Mean $OD_{260/280}$**	**Mean $OD_{260/230}$**
Standard Qiagen procedure	Epithelium	29.45	1.34	0.46
	Stroma	12.47	1.27	0.32
Modifications; 56 ˚C for 1hr	Epithelium	2.90	1.69	0.48
	Stroma	3.15	1.58	0.41
Modifications; 56 ˚C O/N	Epithelium	undetectable		
	Stroma	undetectable		

The concentration of extracted RNA after incubation at 56˚C O/N was undetectable. The concentration of extracted RNA after incubation at 56 ˚C for 1h was very low, but the $OD_{260/280}$ was higher than for RNA extracted with the standard Qiagen protocol and indicated higher RNA purity. A PCR analysis was performed to test the quality of the miRNA in the extracted samples (Table 13).

Table 13. The mean Cq values for miR-23a and miR-191 using template extracted with miRNeasy FFPE kit from Qiagen.

PCR analysis			
Extraction kit	**Tissue section**	**Mean C_q miR-23a**	**Mean C_q miR-191**
Standard Qiagen procedure	Epithelium	33.21	33.55
	Stroma	31.34	33.21
Modifications; 56 ˚C for 1h	Epithelium	30.99	31.18
	Stroma	32.78	32.48
Modifications; 56 ˚C O/N	Epithelium	31.88	31.80
	Stroma	34.83	35.51

The Cq values were high for RNA extracted with both standard Qiagen procedure and modified procedure. Overall, modifications of the protocol did not yield higher amounts of miRNA from microdissected samples. The Cq values for the spike-in controls were acceptable, confirming a successful PCR and that no contaminants were present in the reaction (see appendix 9.2.1).

We also tried to optimize laser microdissection by dissecting the entire area of interest in the section (without separating epithelium and stroma), but the yield and quality of miRNA were still not improved.

4.2 Optimization of methods for extraction of miRNA from macrodissected tissue

An experienced pathologist identified and marked the areas of interest in histological sections from patients included in the study. Macrodissection of the marked area was performed from the FFPE biopsy. The macrodissected sections were deparaffinized and RNA was extracted with miRNeasy FFPE kit from Qiagen. The RNA was further used for measuring expression of miRNA with quantitative PCR. The endogenous reference genes miR-23a and -191 were used.

4.2.1 Optimization of miRNeasy FFPE kit

Modifications of the miRNeasy FFPE kit protocol were made to optimize the yield and purity of total RNA. The sections were incubated at 56 ˚C for 1 hour (1h) due to earlier indications of improved RNA quality on microdissected samples. After conferring with Qiagen support, additional modifications were added to the standard protocol. The spin columns containing RNA were washed three times instead of two and elution was performed in two rounds, where 10 minute incubation was added in the second round. The concentration and purity of the extracted RNA were measured photometrically on Nanodrop.

Table 14. The mean results of quality and yield of extracted RNA with miRNeasy FFPE kit from Qiagen

Photometrical measurements			
Macrodissected samples	**Mean ng/µl**	**Mean $OD_{260/280}$**	**Mean $OD_{260/230}$**
Modified Qiagen procedure	20.52	1.82	0.93

Both the yield and purity of extracted RNA was significantly better on macrodissected tissue (Table 14) than microdissected tissue (Table 12) with a mean concentration of 20.52 ng /µl, mean absorbance at $OD_{260/280}$ of 1.82 and mean absorbance at $OD_{260/230}$ of 0.93. A PCR analysis was performed to test the quality of the miRNA in the extracted samples (Table 15).

Table 15. The mean Cq value for the reference gene miR-23a using template extracted with miRNeasy FFPE kit from Qiagen

PCR analysis	
Macrodissected samples	**Mean C_q miR-23a**
Modifications; 56 ˚C for 1 hour	27.36

Cq values obtained from the following PCR analysis were much lower and stable for macrodissected tissue (Table 15), as compared to microdissected tissue (Table 13). A mean Cq of 27.36 of the reference gene, show that the amount of miRNA is acceptable. The concentration of miRNA was further investigated on Bioanalyzer 2100.

The small RNA kit was used to analyze in the total RNA extracted from 10 macrodissected samples and measure the proportion of small RNAs. Six of the samples were normal cervical samples and four of the samples were CIN3 lesions (Table 16). The kit defines small RNA as RNA fragments with a size of 0–150 nt, whereas miRNA is defined as RNA fragments with a size of 15–40 nt.

Table 16. The mean concentration of small RNA and miRNA.

Electrophoretic measurements		
Macrodissected samples	**Mean small RNA conc. [ng/µl]**	**Mean small miRNA conc. [ng/µl]**
Normal cervical samples	8 757300	3 603400
CIN3 samples	113 199100	22 009000

The result obtained from the small RNA kit by the use of Bioanalyzer 2100, revealed that the macrodissected samples contained small amounts of miRNA. Higher quantities of miRNA were found in CIN3 samples. With good quality miRNA, a distinct peak should be detectable within the miRNA region (15–40 nt). No distinct peak was detected for any of the samples (Figure 17).

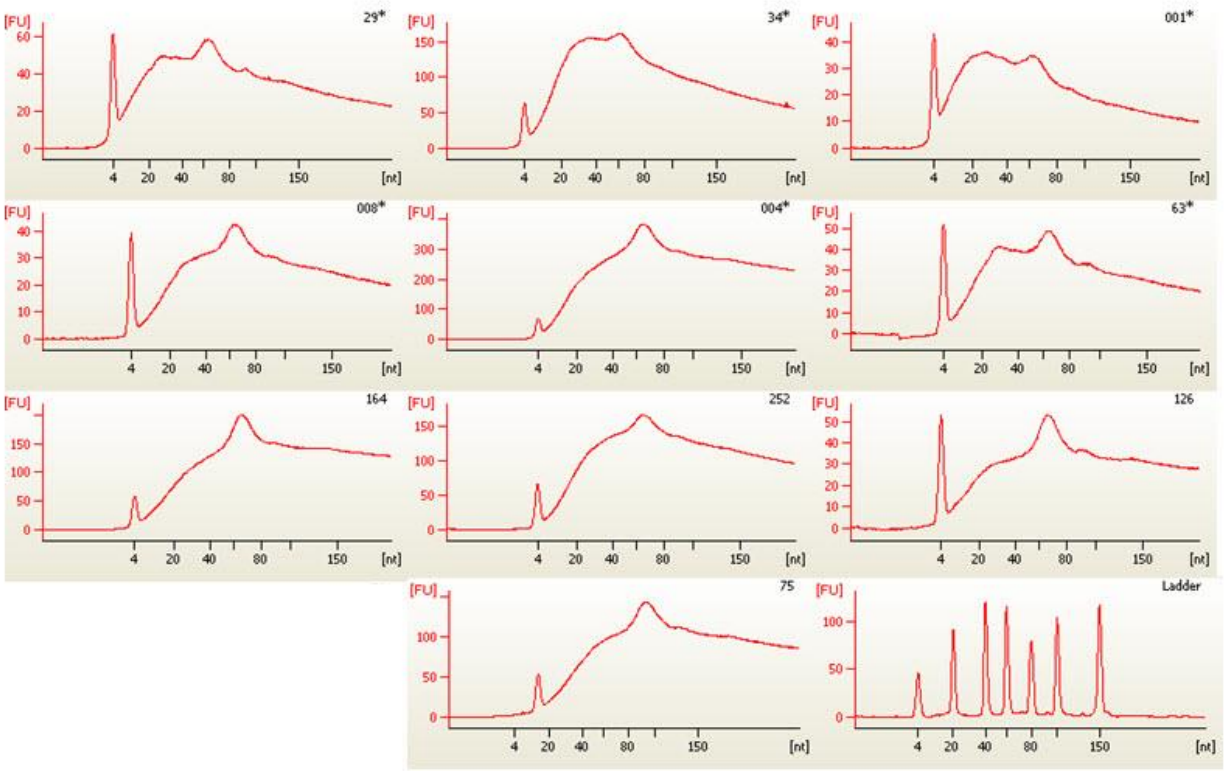

Figure 17. The electropherogram show the result obtained from the analysis of 10 samples. Normal samples are marked with *. Fluorescence is shown on the y-axis and amount of nucleotides is shown on the x-axis. The ladder is shown in the electropherogram at the bottom right lane.

4.3 Expression of miR-18a and miR-18b by RT-qPCR

RT-qPCR analysis was performed to compare the expression of miR-18a and miR-18b in HPV-16 positive CIN3 lesions and normal cervical tissue. For 20 samples with CIN3 lesions and 18 samples with normal cervical tissue, the quality of RNA was sufficient for PCR. Negative and positive quality control in each PCR run were approved.

To determine the relative expression of each target gene, a comparative Cq method was performed. Cq values of the target gene (miR-18a and -18b) were normalized by endogenous reference genes (miR-23a and -191). Since two different reference genes were used, mean differences between these were calculated and used for normalization in further analysis:

$$\Delta Cq = Cq\ (sample) – Cq\ (mean\ difference\ reference\ genes)$$

The relative expression of each target gene is calculated by the following equation;

$$2^{-\Delta Cq}$$

Normality of distribution of the samples was investigated. We concluded that the sample variance was equal. An independent sample t-test was used to determine differences in the PCR for miR-18a and -18b in 20 CIN3 lesions versus 18 normal cervical tissues. The distribution of miR-18a and -18b is presented in boxplots (Figure 18 and Figure 19).

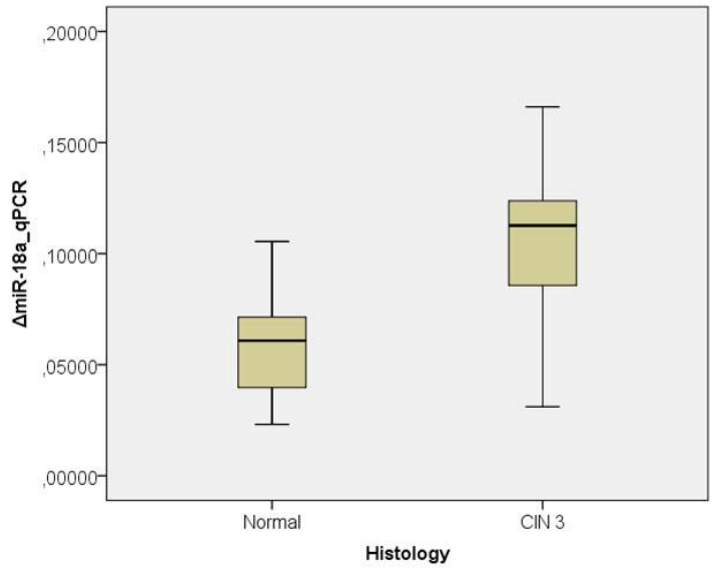

Figure 18. Distribution of miR-18a in 18 normal cervical tissues and 20 HPV-16 positive CIN3 lesions.

Figure 18 shows the distribution of relative quantity of miR-18a in normal cervical tissue and CIN3 lesions. There is a wide distribution of results in the CIN3 group, but more than 50 % of the CIN3 samples have higher quantities of miR-18a than normal cervical samples. Independent t-test showed significant differences for the CIN3 group versus the normal group ($p<0.001$) and 95 % confidence intervals for the mean difference ranged 0.024–0.063 (Table 17).

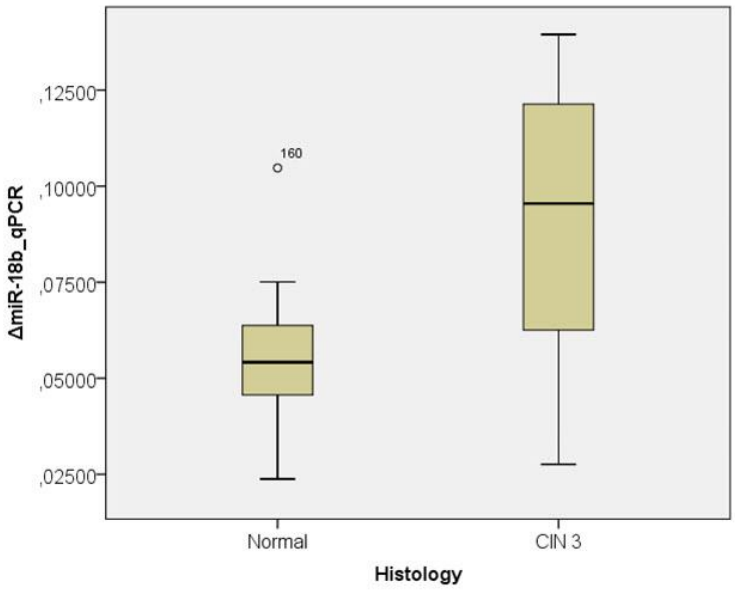

Figure 19. Distribution of miR-18b in 18 normal cervical tissues and 20 HPV-16 positive CIN3 lesions.

Figure 19 shows the distribution of relative quantity of miR-18b in normal cervical tissue and in CIN3 lesions. An outlier (160) with higher expression than expected is seen in the normal group. There is a wide distribution of results in the CIN3 group, but a higher quantity of miR-18b is found in more than 50 % of CIN3 samples as compared to normal cervical tissue. Independent t-test showed significant differences for the CIN3 group versus normal group ($p<0.001$) and 95 % confidence intervals for the mean difference ranged 0.019–0.055 (Table 17).

Table 17. Independent samples t-test between 20 HPV-16 positive CIN3 lesions and 18 normal cervical lesions.

Independent Samples t-test					
qPCR	Sig. (2-tailed)	Mean Difference	Std. Error Difference	95% Confidence Interval of the Difference	
				Lower	Upper
CIN3 lesions vs. normal cervical tissue, miR-18a	.000	.04380336	.00977099	.02398687	.06361984
CIN3 lesions vs. normal cervical tissue, miR-18b	.000	.03735307	.00893388	.01923431	.05547183

4.4 Visualization of miR-18a and miR-18b by CISH

CISH was performed on HPV-16 positive CIN3 lesions for visualization of miR-18a and miR-18b *in situ*. For 18 CIN3 lesions an area with normal tissue was suitable for visualization. Prior to performing CISH, histological sections from the FFPE tissue were analyzed by a diagnostic pathologist, who identified and marked the dysplastic area. CISH results were measured by semi-quantitative scoring by two different observers blinded for each other's results. Positive cells were counted in CIN3 versus normal tissue within the same biopsy. For results with small discrepancies the mean value from the two observers were calculated. For 75 % of the samples there was an agreement between the observers. For results with larger discrepancies, with more than 35 %, a consensus was done. A paired sample t-test was used

to determine significant differences for miR-18a and -18b between CIN3 lesions and normal cervical tissue. The distribution of miR-18a and -18b is presented in Boxplots (Figure 20 and Figure 22).

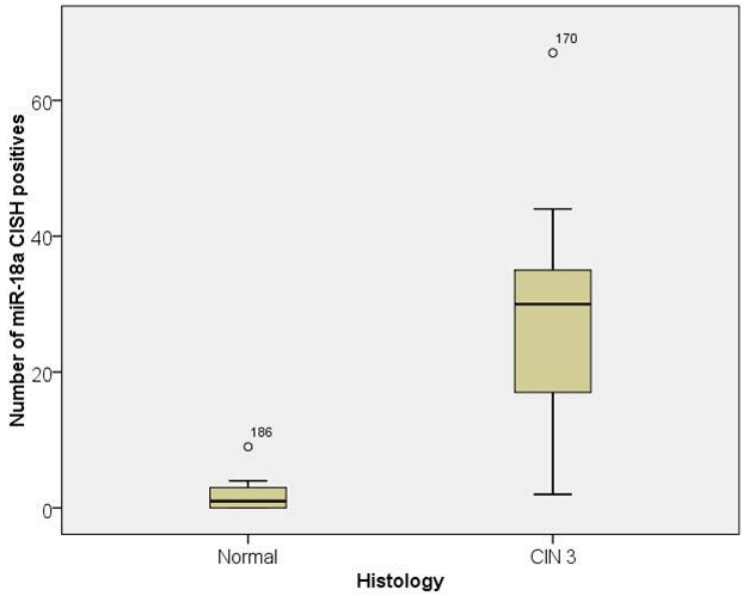

Figure 20. Distribution of miR-18a positive cells in CIN3 versus normal tissue within the same biopsy.

Figure 20 shows the distribution of CISH positive miR-18a in CIN3 lesions versus normal cervical tissue within the same samples. Outliers with high expression are seen in both the normal group (186) and the CIN3 group (170). There is a wide range in distribution of miR-18a CISH positives in the CIN3 group, compared to the normal group. For the vast majority of samples, much higher quantities of miR-18a were found in the CIN3 lesions, compared to the normal cervical areas. This is visually demonstrated in Figure 21. Paired samples t-test showed significant differences between semi-quantitative CIN3 lesions and normal cervical area ($p<0.001$), and 95 % confidence intervals for the mean difference ranged from 19.92–39.74 (Table 18).

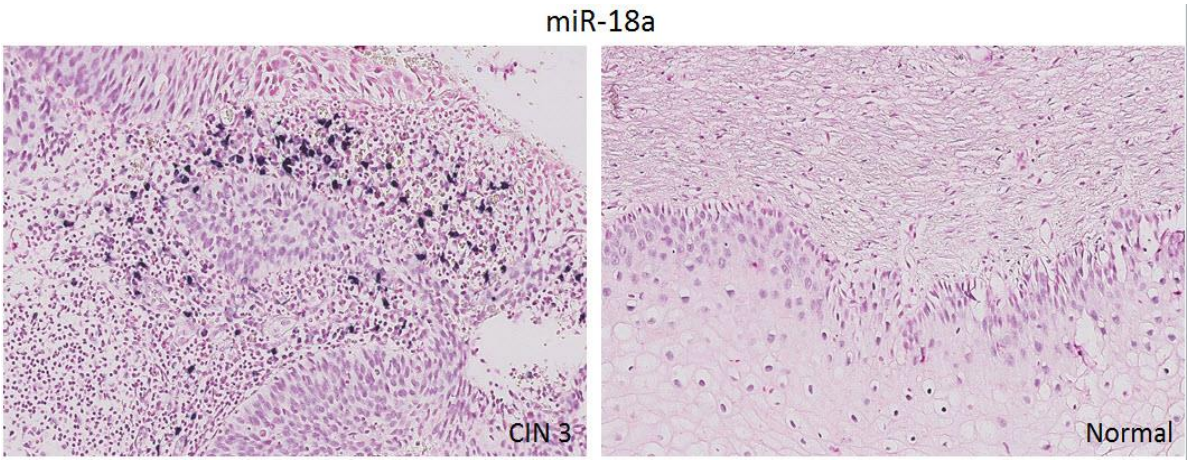

Figure 21. Semi-quantitiative scoring of miR-18a (blue color) in a CIN3 area versus a normal cervical area. High numbers of miRNAs were observed in stroma around the area of CIN, and few or none miRNAs were observed in stroma of normal cervical tissue (20x).

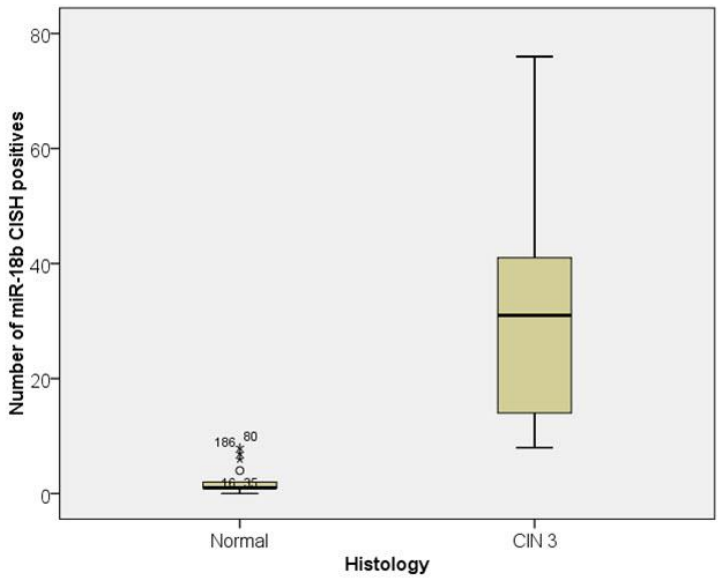

Figure 22. Distribution of miR-18b positive cells in CIN3 versus normal tissue within the same biopsy.

Figure 22 shows the distribution of CISH positive miR-18b in CIN3 lesions versus normal cervical tissue within one sample. Several outliers (16, 35, 80, 186) with high expression is seen in the normal group. There is a wide range in distribution of CISH positive miR-18b in the CIN3 group, compared to normal group. A much higher quantity of miR-18b is found in the CIN3 lesions, compared to the normal cervical areas. This is visually demonstrated in Figure 23. Paired samples t-test showed significant differences between CIN3 lesions and

normal cervical area (p<0.001), and 95 % confidence intervals for the mean difference ranged from 16.91–46.21 (Table 18).

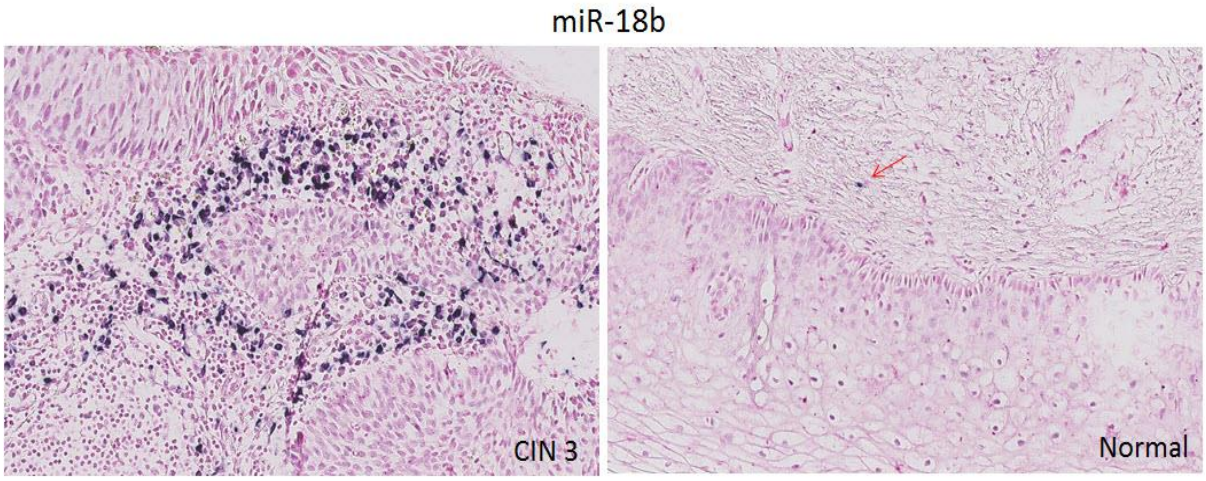

Figure 23. Semi-quantitiative scoring of miR-18b (blue color) in CIN3 area versus normal cervical area. High numbers of miRNAs were observed in stroma around the area of CIN, and few or none miRNAs were observed in stroma of normal cervical tissue (20x magnification).

Table 18. Paired sample t-test of CISH positive scores (miR-18a and -18b) for CIN3 versus normal cervical tissue.

Paired Samples Test						
CISH	Mean	Std. Deviation	Std. Error Mean	95% Confidence Interval of the Difference		Sig. (2-tailed)
				Lower	Upper	
CIN3 versus normal miR-18a	29.833	19.930	4.698	19.922	39.744	.000
CIN3 versus normal miR-18b	31.556	29.458	6.943	16.906	46.205	.000

5 Discussion

The aim of this thesis was to optimize methods for isolation, purification and detection of miR-18a and miR-18b in FFPE cervical specimens. We wanted to compare the expression of miR-18a and -18b in persistent HPV-16 positive CIN3 samples and normal cervical samples by the use of RT-qPCR and semi-quantitative scoring with CISH.

5.1 Optimization of methods

The first part of this study consisted of optimizing methods for detection of miR-18a and -18b in FFPE tissue from HPV-16 positive CIN3 samples and normal cervical lesions. Our main goal was to optimize miRNA yield obtained from laser microdissected (LMD) tissue. LMD is a very accurate method making it easy to collect specific cells from different areas in a biopsy. The PCR analysis in this study is performed with primers for the reference genes miR-23a and miR-191. These reference genes have been identified as stable reference genes for normalization in profiling studies of cervical tissue. Their expression was shown to be stable for normal, dysplastic and cancer tissue [55]. The use of standard reference genes for normalization is important to increase the reliability and reproducibility of the experiment [112]. MiRNAs are very tissue-specific and may vary significantly across different samples. The reference genes should have similar properties as the target gene, and it is important that the expression of the reference gene do not differ between normal and tumor tissue of interest.

We started comparing two kits to see which yielded the most satisfactory purity of miRNA. By measuring the concentration photometrically, High Pure FFPET RNA isolation kit from Roche yielded higher amounts of total RNA than miRNeasy FFPE kit from Qiagen. The ratio of $OD_{260/280}$ and $OD_{260/230}$ should preferably be larger or equal to 1.80 to conclude satisfactory purity of isolated RNA. In this material lower ratios were expected, as FFPE tissue often is degraded, but it may still function well for PCR. Photometrical methods do not allow discrimination between different fractions of RNA. Thus, a PCR analysis, with reference gene miR-191, was performed to test the quality of the miRNA in the extracted samples. The PCR analysis revealed that even though both kits yielded unsatisfactory concentrations of miRNA, the miRNeasy FFPE kit yielded the best RNA quality for amplification and qPCR detection of

miRNA (Table 11). The High Pure FFPET RNA isolation kit from Roche had been tested in an earlier study (unpublished data) without giving satisfactory results. Taking this into consideration together with the results we achieved, we decided not to use this kit for further optimization.

miRNeasy FFPE kit was therefore chosen for further optimization for isolation of RNA from microdissected tissue. Modifications were made by changing one of the heating steps in the standard protocol. Proteinase K break protein bonds, while high temperatures break the cross bindings between proteins and nucleic acids. According to standard protocol incubation at 85 ˚C for 15 minutes is sufficient for breaking cross links. In attempt to increase the RNA yield, the digestion time with proteinase K at 56 ˚C was extended from 15 minutes to 1 hour (1h) and also overnight (O/N) [118]. Measurements on Nanodrop showed that the concentration of extracted RNA after incubation overnight was too low to detect. We suspect that the incubation process was too long leading to degradation of RNA. The concentration of extracted RNA that had been incubated for 1 hour was also very low, but the ratio of $OD_{260/280}$ was higher than for RNA extracted with standard procedure. Higher ratio of $OD_{260/280}$ indicates higher purity of RNA. The PCR analysis revealed that the Cq values were high showing that the quality and amount of the extracted RNA was still unsatisfactory.

There may be several reasons for the low concentration and purity of miRNA extracted after LMD. First of all, the amount of material obtained from LMD is limited. Second, FFPE tissue can be challenging to work with. Before the tissue has been thoroughly fixed in the formalin, the DNA and RNA have started to degrade. This will cause limitations for the size of RNA fragments that are possible to detect in FFPE material. FFPE fixation will also cause protein cross-linking and this can be challenging for extraction of high purity RNA. On the other hand, miRNA has been shown to be more stable in FFPE tissue than longer RNA sequences such as mRNA. Li *et al.* showed that the amount of miRNA in total RNA was greater in FFPE tissue than in snap frozen tissue, when the input amounts of RNA were the same [119]. One reason of their stable expression in FFPE tissue is that miRNA are short, only 22 nucleotides, thus they will not degrade as easily as longer RNAs. Other possible explanations may be their lack of structure, lack of specific target sequence or that they often are protected in a complex such as miRISC [88, 90]. Another issue is that the tissue sections were stained with cresyl violet prior to LMD for better visualization of the cells. The staining may interfere with

the RNA, and thus, affect the yield of RNA after extraction [90, 91]. The impact of the laser beam itself and the fact that the tissue is subjected to room temperature for an extended period of time, may also expedite the RNA degradation process [90]. The sensitivity of the PCR analysis may have been improved by adding a preamplification step, but for this experiment we decided to use macrodissected tissue instead for the rest of the study.

The tissue area of interest was cut on a microtome. The standard protocol for the miRNeasy FFPE kit, was modified. Modifications included extended incubation time for 1 hour at 56 ˚C, an additional washing step and prolonged incubation time during elution. The concentration and purity of the extracted RNA were measured on Nanodrop and on Bioanalyzer. The concentration and purity of RNA was significantly better when extracting RNA from macrodissected tissue. The ratio of $OD_{260/280}$ was satisfactory, but the ratio of $OD_{260/230}$ was low (Table 14). The low ratio of $OD_{260/230}$ is probably a result of absorbance of organic compounds, indicating that the samples still contains residual phenol, guanidine and/or alcohol from the RNA extraction.

In the results obtained from the Bioanalyzer, no distinct peak for miRNA was obtained for any of the samples. A reasonable explanation can be that the RNA fragments are degraded prior to and under formalin fixation. In addition, deparaffinization and extraction procedures may have an impact on degradation. FFPE material will therefore have an increased proportion of small RNAs including both miRNA and fragmented RNA. This is an explanation for the curves observed after electrophoresis with the Bioanalyzer, where a distinct peak is not observed, but rather a gradually declining slope (Figure 17) [98]. A PCR analysis with primers for the reference genes revealed that the Cq values were lower and also more stable in the macrodissected tissue. The Cq values were also quite similar for dysplastic tissue as compared to normal. We concluded that macrodissected tissue yields greater amounts of RNA than microdissected tissue. Macrodissection is not as accurate as laser microdissection, since the marked area is cut by a microtome, and not by a UV laser. Still, we concluded that the amount and purity of miRNA was sufficient for further analysis (Table 15).

5.2 Detection of miR-18a and miR-18b

RT-qPCR analysis was performed to compare the expression of miR-18a and miR-18b in HPV-16 positive CIN3 lesions and normal cervical tissue, from macrodissected FFPE tissue. Both miR-18a and -18b were upregulated in CIN3 lesions as compared to normal cervical tissue. In the 25 % quartile there was an overlap between the CIN3 group and the normal group, but for the majority of samples a higher quantity of miR-18a were found in CIN3 lesions (Figure 18). The distribution of miR-18b in the CIN3 group had a much wider range compared to miR-18a. In addition one of the patient samples with normal cervical tissue (160) had higher expression than expected, but an possible explanation for this is not obvious. For the majority of the samples, a higher quantity of miR-18b was found in CIN3 lesions as compared to the normal samples (Figure 19). An independent t-test confirmed the significant differences between CIN3 lesions and normal cervical tissue in miR-18a ($P < 0.001$) and -18b ($P < 0.001$) (Table 17).

CISH was performed for visualization of expression of miR-18a and miR-18b in cervical tissue. Clusters of CISH positive miR-18a and -18b were found in the stroma close to the high grade CIN lesions, but not in the epithelial lesions (Figure 21 and Figure 23). For 18 CIN3 lesions, a comparison between normal and dysplastic tissue within the same sample was possible. A boxplot of the miR-18a CISH positives showed a much higher and wider distribution of miR-18a positives in the CIN3 group as compared to the normal group (Figure 20). In addition, one of the patient samples with normal cervical tissue (186) had higher expression than expected, but an possible explanation for this was not obvious. A boxplot of the miR-18b CISH positives showed a high and wide range in distribution of miR-18b in the CIN3 group, as compared to the normal group. Several outliers were observed in both the CIN3 group (170, 252) and in the normal group (35, 80, 160, 186), indicating high variety between samples (Figure 22). High expression of miR-18a and -18b was found in virtually all CIN3 lesions, but not in the normal cervical tissue, as demonstrated in Figure 21 and Figure 23. A paired samples t-test confirmed the significant differences between CIN3 lesions and normal cervical tissue in both miR-18a ($P < 0.001$) and -18b ($P < 0.001$) (Table 18).

Quantitation with RT-qPCR analysis is a more accurate method than semi-quantitative scoring of CISH positives. Counting CISH positive cells is a subjective procedure and may not

be very reproducible. The tissue collected for RNA extraction from CIN3 lesions was from the same area as the semi-quantification of CISH positives. An area with normal tissue in the same sample as the CIN3 tissue was used to quantify CISH positives in normal epithelium. For RNA extraction of normal tissue, independent patient samples with normal biopsies were used. The wide distribution of results in the CIN3 group are most likely due to biological factors such as natural genetic variation, time duration of HPV infection prior to biopsy removal, aging and other health problems. These are all factors affecting individual immune response and may contribute to variation between samples.

Results obtained from CISH showed that the expression of miR-18a and -18b is much higher in the microenvironment of CIN3 as compared to normal cervix (Figure 21 and Figure 23) The results are confirmed by paired samples t-test (Table 18). Results obtained with qPCR also showed significant differences between miR-18a and -18b in CIN3 lesions as compared to normal cervix. Since RNA was extracted from macrodissected whole sections, we cannot conclude whether the miRNAs in question originate only from the stroma or from both epithelium and stroma.

miR-18a is a member of the miR-17-92 cluster which has been found to be a modulator of effector and memory T-cells. The expression of miR-17-92 is critical for rapid expansion of CD8+ T-cells [120]. However, high expression of miR-17-92 differentiates CD8+ T-cells toward short-lived terminal effector cells by enhancing the mammalian target of rapamycin (mTOR) [121]. The mTOR controls proliferation, cell growth and survival and is often upregulated in cancer [122]. A continued excessive expression of miR-17-92 leads to a gradual loss of memory cells and memory differentiation of CD8+ T-cells [120, 121]. The CD8+ T-cells are critical for clearance of HPV-associated lesions. High-risk HPV can impair the CD8+ T-cells, which lead to persistence of the HPV infection and further development of the lesion into a higher grade lesion or even into cancer [46].

In breast cancer studies miR-18a and -18b have been found to directly target and inhibit oestrogen-α (ER-α) signaling [69, 70]. A study conducted by Jonsdottir *et al.* showed highly significant association between high expression of miR-18a and -18b and oestrogen receptor negativity, in addition to high proliferation and cytokeratin 5/6 positivity [71]. In a cervical cancer cell-line study, miR-18a was found to have an important role in latent TGF-β1

feedback loop and in this way controlling the cytostatic response to TGF-β. Also, miR-24 was found to cooperate with miR-18a in this process [74].

We investigated the expression of miR-18a and -18b in cervical tissue and found that miR-18a and -18b are highly upregulated in persistent CIN3 lesions. High expression of these miRNAs might be a sign for bad prognosis of a lesion with potential for developing into cancer. Interestingly, CISH revealed that these miRNAs are heavily expressed in the microenvironment the of CIN3 lesions. The cytotoxic T-cells are important for eradication of HPV infected cells and cancer development. We wanted to investigate if the miRNAs were expressed adjacent to T lymphocytes. A visualized comparison between CD8+ T-cells and miR-18a expression in the same area of a CIN3 dysplasia was performed. The impression was that miR-18a correlated with CD8+ T-cells (Figure 24). Earlier studies have shown that the composition of immune cells in the microenvironment of CIN3 lesions is an important factor for regression of high grade lesions [25].

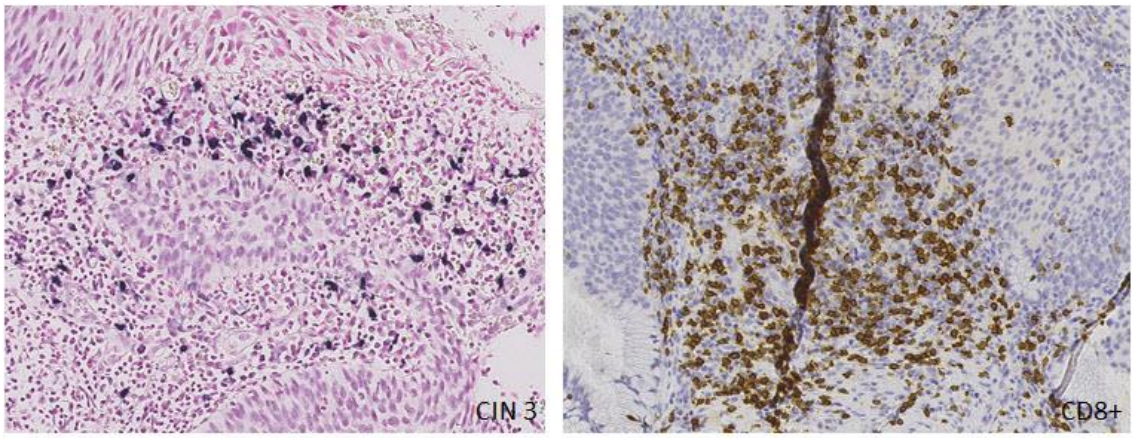

Figure 24. Comparison between miR-18a expression and CD8+ staining within the same area in a histological section (20x).

6 Conclusion

We have shown that miR-18a and miR-18b are highly expressed in persistent HPV-16 positive CIN3 lesions versus normal cervical tissue. With two different methods we showed that the differences were significant. This may indicate that high expression of miR-18a and -18b is a sign of poor prognosis for a lesion with potential to develop into cancer. A visualized comparison between CD8+ T-cells and miR-18a expression in the same area of a CIN3 dysplasia, showed a possible relationship between the cytotoxic T-cells and the miRNAs in question. Importantly, miR-18a is a member of the miR-17-92 cluster, shown to be a modulator of effector cells. We therefore hypothesize that high numbers of miR-18a may down-regulate expression of effector CD8+ cells.

7 Future perspective

The future perspective is to study the expression of miR-18a and miR-18b in regressing CIN3 lesions with RT-qPCR and CISH. A comparison of the results obtained from persistent, regressive and normal cervical tissue may reveal if these miRNAs potentially can serve as markers for regression. Double staining with CISH and immunohistochemistry may give a better answer as to whether there is a relationship between miR-18a, miR-18b and CD8+ T-cells in CIN3. Functional analysis with inhibitors for miR-18a, -18b and -24 in cervical cancer cell line cultures is another future perspective. This may give new insight to the function of these miRNAs in development of cervical cancer.

8 References

1. Vici, P., et al., *Emerging Biological Treatments for Uterine Cervical Carcinoma.* J Cancer, 2014. **5**(2): p. 86-97.
2. Larønningen S, L.I., Møller B, Engholm G, Storm HH, Johannesen TB, *NORDCAN – Cancer data from the Nordic countries*. 2013, Cancer Registry of Norway: Oslo. p. 28-29.
3. Cancer, I.A.f.R.o. *Cervical Cancer; Estimated Incidence, Mortality and Prevalence Worldwide in 2012*. 2012 [cited 2014 29.04]; Available from: http://globocan.iarc.fr/Pages/fact_sheets_cancer.aspx.
4. Shepherd, J.H., *Cervical cancer.* Best Pract Res Clin Obstet Gynaecol, 2012. **26**(3): p. 293-309.
5. Nygard, M., *Screening for cervical cancer: when theory meets reality.* BMC Cancer, 2011. **11**: p. 240.
6. Skare, G.B., Lönnberg, S. *The annual report for 2012: cervical cancer screening programme*. 2012 [cited 2014 29.04]; Available from: http://www.kreftregisteret.no/Global/Publikasjoner%20og%20rapporter/Livmorhalskreft/aarsrapport_livmorhals_2012.pdf.
7. Sigurdsson, K., *The Icelandic and Nordic cervical screening programs: trends in incidence and mortality rates through 1995.* Acta Obstet Gynecol Scand, 1999. **78**(6): p. 478-85.
8. Miller, A.B., et al., *Report on a Workshop of the UICC Project on Evaluation of Screening for Cancer.* Int J Cancer, 1990. **46**(5): p. 761-9.
9. Vogelstein, B. and K.W. Kinzler, *The Genetic Basis of Human Cancer*. 2002: McGraw-Hill, Medical Pub. Division. 689-95.
10. Schiffman, M., et al., *Human Papillomavirus Testing in the Prevention of Cervical Cancer.* Journal of the National Cancer Institute, 2011. **103**(5): p. 368-383.
11. Kim, J.J., et al., *Modeling cervical cancer prevention in developed countries.* Vaccine, 2008. **26 Suppl 10**: p. K76-86.
12. Tota, J.E., et al., *The road ahead for cervical cancer prevention and control.* Curr Oncol, 2014. **21**(2): p. e255-e264.
13. Health, N.I.o.P. *HPV-vaccination (Human papillomavirus)*. 2008 [cited 2014 30.04]; Available from: http://www.fhi.no/eway/default.aspx?pid=239&trg=Content_6493&Main_6157=6287:0:25,5501&MainContent_6287=6493:0:25,6826&Content_6493=6441:69803::0:6446:9:::0:0#eHandbook698031.
14. Roden, R. and T.C. Wu, *How will HPV vaccines affect cervical cancer?* Nat Rev Cancer, 2006. **6**(10): p. 753-63.
15. Cheung, T.H., et al., *Dysregulated microRNAs in the pathogenesis and progression of cervical neoplasm.* Cell Cycle, 2012. **11**(15): p. 2876-84.
16. Baak, J.P., et al., *Dynamic behavioural interpretation of cervical intraepithelial neoplasia with molecular biomarkers.* J Clin Pathol, 2006. **59**(10): p. 1017-28.
17. Barakat, R.R., Markman, M., Randall, M, *Principles and Practice of Gynecologic Oncology*. 2009, Philadelphia: Lippincott Williams & Wilkins. 523-24.
18. Oparka, R., et al., *Human papillomavirus infection and its association with neoplasia*, in *Small DNA tumour viruses*, K. Gaston and K. Gaston, Editors. 2012, Caister Academic Press: Wymondham. p. 1-18.
19. N Golet, A., *Unified terminology for pathology of the cervix.* Bulletin of the World Health Organization, 2000. **78**: p. 146-146.
20. Apgar, B.S., L. Zoschnick, and T.C. Wright, Jr., *The 2001 Bethesda System terminology.* Am Fam Physician, 2003. **68**(10): p. 1992-8.
21. Herbert, A., et al., *European guidelines for quality assurance in cervical cancer screening: recommendations for cervical cytology terminology.* Cytopathology, 2007. **18**(4): p. 213-9.

22. Schmitt, M., et al., *Multiple human papillomavirus infections with high viral loads are associated with cervical lesions but do not differentiate grades of cervical abnormalities.* J Clin Microbiol, 2013. **51**(5): p. 1458-64.
23. Sari Aslani, F., et al., *Evaluation of Ki67, p16 and CK17 Markers in Differentiating Cervical Intraepithelial Neoplasia and Benign Lesions.* Iran J Med Sci, 2013. **38**(1): p. 15-21.
24. Uleberg, K.E., et al., *A protein profile study to discriminate CIN lesions from normal cervical epithelium.* Cell Oncol (Dordr), 2011. **34**(5): p. 443-50.
25. Ovestad, I.T., et al., *Local immune response in the microenvironment of CIN2-3 with and without spontaneous regression.* Mod Pathol, 2010. **23**(9): p. 1231-40.
26. Munk, A.C., et al., *Consistent condom use increases the regression rate of cervical intraepithelial neoplasia 2-3.* PLoS One, 2012. **7**(9): p. e45114.
27. Kyrgiou, M., et al., *Obstetric outcomes after conservative treatment for intraepithelial or early invasive cervical lesions: systematic review and meta-analysis.* Lancet, 2006. **367**(9509): p. 489-98.
28. Bruinsma, F.J. and M.A. Quinn, *The risk of preterm birth following treatment for precancerous changes in the cervix: a systematic review and meta-analysis.* BJOG, 2011. **118**(9): p. 1031-41.
29. Uleberg, K.E., et al., *Discrimination of grade 2 and 3 cervical intraepithelial neoplasia by means of analysis of water soluble proteins recovered from cervical biopsies.* Proteome Sci, 2011. **9**: p. 36.
30. Thomison, J., 3rd, L.K. Thomas, and K.R. Shroyer, *Human papillomavirus: molecular and cytologic/histologic aspects related to cervical intraepithelial neoplasia and carcinoma.* Hum Pathol, 2008. **39**(2): p. 154-66.
31. Stanley, M., *Pathology and epidemiology of HPV infection in females.* Gynecol Oncol, 2010. **117**(2 Suppl): p. S5-10.
32. Bernard, H.U., et al., *Classification of papillomaviruses (PVs) based on 189 PV types and proposal of taxonomic amendments.* Virology, 2010. **401**(1): p. 70-9.
33. Middleton, K., et al., *Organization of human papillomavirus productive cycle during neoplastic progression provides a basis for selection of diagnostic markers.* J Virol, 2003. **77**(19): p. 10186-201.
34. Doorbar, J., et al., *The biology and life-cycle of human papillomaviruses.* Vaccine, 2012. **30 Suppl 5**: p. F55-70.
35. Burchell, A.N., et al., *Chapter 6: Epidemiology and transmission dynamics of genital HPV infection.* Vaccine, 2006. **24 Suppl 3**: p. S3/52-61.
36. Wang, X., et al., *Human semen: the biological basis of sexual behaviour to promote human papillomavirus infection and cervical cancer.* Med Hypotheses, 2010. **74**(6): p. 1015-6.
37. Cid-Arregui, A., *Therapeutic vaccines against human papillomavirus and cervical cancer.* Open Virol J, 2009. **3**: p. 67-83.
38. Staff, I.A.f.R.o.C., *IARC Monographs on the Evaluation of Carcinogenic Risks to Humans. Volume 90: Human papillomaviruses*. 2007, World Health Organization (WHO): Albany, NY, USA. p. 47.
39. zur Hausen, H., *Papillomaviruses and cancer: from basic studies to clinical application.* Nat Rev Cancer, 2002. **2**(5): p. 342-50.
40. Doorbar, J., *The papillomavirus life cycle.* J Clin Virol, 2005. **32 Suppl 1**: p. S7-15.
41. Moody, C.A. and L.A. Laimins, *Human papillomavirus oncoproteins: pathways to transformation.* Nat Rev Cancer, 2010. **10**(8): p. 550-60.
42. Leto, M., et al., *Human papillomavirus infection: etiopathogenesis, molecular biology and clinical manifestations.* An Bras Dermatol, 2011. **86**(2): p. 306-17.
43. Oh, S.T., M.S. Longworth, and L.A. Laimins, *Roles of the E6 and E7 proteins in the life cycle of low-risk human papillomavirus type 11.* J Virol, 2004. **78**(5): p. 2620-6.
44. Pecorino, L., *Molecular Biology Of Cancer: Mechanisms, Targets, And Therapeutics*. 2005: Oxford University Press, Incorporated. 111-13.

45. Tristram, A. and A. Fiander, *Human papillomavirus (including vaccines).* Obstetrics, Gynaecology and Reproductive Medicine, 2007. **17**(11): p. 324-329.
46. Stanley, M., *Immune responses to human papillomavirus.* Vaccine, 2006. **24 Suppl 1**: p. S16-22.
47. Guess, J.C. and D.J. McCance, *Decreased migration of Langerhans precursor-like cells in response to human keratinocytes expressing human papillomavirus type 16 E6/E7 is related to reduced macrophage inflammatory protein-3alpha production.* J Virol, 2005. **79**(23): p. 14852-62.
48. Munk, A.C., et al., *Interaction of epithelial biomarkers, local immune response and condom use in cervical intraepithelial neoplasia 2-3 regression.* Gynecol Oncol, 2012. **127**(3): p. 489-94.
49. Nelson, D.L.C.M.M.L.A.L., *Lehninger, principles of biochemistry*. 2008, New York: W. H. Freeman and Company.
50. Lee, R.C., R.L. Feinbaum, and V. Ambros, *The C. elegans heterochronic gene lin-4 encodes small RNAs with antisense complementarity to lin-14.* Cell, 1993. **75**(5): p. 843-54.
51. Reinhart, B.J., et al., *The 21-nucleotide let-7 RNA regulates developmental timing in Caenorhabditis elegans.* Nature, 2000. **403**(6772): p. 901-6.
52. Lee, R.C. and V. Ambros, *An extensive class of small RNAs in Caenorhabditis elegans.* Science, 2001. **294**(5543): p. 862-4.
53. Pereira, P.M., et al., *MicroRNA expression variability in human cervical tissues.* PLoS One, 2010. **5**(7): p. e11780.
54. Guo, H., et al., *Mammalian microRNAs predominantly act to decrease target mRNA levels.* Nature, 2010. **466**(7308): p. 835-40.
55. Shen, Y., et al., *Identification of miR-23a as a novel microRNA normalizer for relative quantification in human uterine cervical tissues.* Exp Mol Med, 2011. **43**(6): p. 358-66.
56. Beezhold, K.J., V. Castranova, and F. Chen, *Microprocessor of microRNAs: regulation and potential for therapeutic intervention.* Mol Cancer, 2010. **9**: p. 134.
57. SIGMA-ALDRICH. *miRNA (microRNA) introduction*. Retrieved 25.03.14; Available from: http://www.sigmaaldrich.com/life-science/functional-genomics-and-rnai/mirna/learning-center/mirna-introduction.html.
58. Denli, A.M., et al., *Processing of primary microRNAs by the Microprocessor complex.* Nature, 2004. **432**(7014): p. 231-5.
59. Zheng, Z.M. and X. Wang, *Regulation of cellular miRNA expression by human papillomaviruses.* Biochim Biophys Acta, 2011. **1809**(11-12): p. 668-77.
60. Lee, Y., et al., *Drosha in primary microRNA processing.* Cold Spring Harb Symp Quant Biol, 2006. **71**: p. 51-7.
61. Nishihara, T., et al., *miRISC recruits decapping factors to miRNA targets to enhance their degradation.* Nucleic Acids Res, 2013. **41**(18): p. 8692-705.
62. Sassen, S., E.A. Miska, and C. Caldas, *MicroRNA: implications for cancer.* Virchows Arch, 2008. **452**(1): p. 1-10.
63. Calin, G.A., et al., *Frequent deletions and down-regulation of micro- RNA genes miR15 and miR16 at 13q14 in chronic lymphocytic leukemia.* Proc Natl Acad Sci U S A, 2002. **99**(24): p. 15524-9.
64. He, L., et al., *A microRNA polycistron as a potential human oncogene.* Nature, 2005. **435**(7043): p. 828-33.
65. O'Donnell, K.A., et al., *c-Myc-regulated microRNAs modulate E2F1 expression.* Nature, 2005. **435**(7043): p. 839-43.
66. Tao, J., et al., *microRNA-18a, a member of the oncogenic miR-17-92 cluster, targets Dicer and suppresses cell proliferation in bladder cancer T24 cells.* Mol Med Rep, 2012. **5**(1): p. 167-72.
67. Olive, V., I. Jiang, and L. He, *mir-17-92, a cluster of miRNAs in the midst of the cancer network.* Int J Biochem Cell Biol, 2010. **42**(8): p. 1348-54.

68. Mogilyansky, E. and I. Rigoutsos, *The miR-17/92 cluster: a comprehensive update on its genomics, genetics, functions and increasingly important and numerous roles in health and disease.* Cell Death Differ, 2013. **20**(12): p. 1603-14.
69. Leivonen, S.K., et al., *Protein lysate microarray analysis to identify microRNAs regulating estrogen receptor signaling in breast cancer cell lines.* Oncogene, 2009. **28**(44): p. 3926-36.
70. Yoshimoto, N., et al., *Distinct expressions of microRNAs that directly target estrogen receptor alpha in human breast cancer.* Breast Cancer Res Treat, 2011. **130**(1): p. 331-9.
71. Jonsdottir, K., et al., *Validation of expression patterns for nine miRNAs in 204 lymph-node negative breast cancers.* PLoS One, 2012. **7**(11): p. e48692.
72. Kloth, J.N., et al., *Substantial changes in gene expression of Wnt, MAPK and TNFalpha pathways induced by TGF-beta1 in cervical cancer cell lines.* Carcinogenesis, 2005. **26**(9): p. 1493-502.
73. Annes, J.P., J.S. Munger, and D.B. Rifkin, *Making sense of latent TGFbeta activation.* J Cell Sci, 2003. **116**(Pt 2): p. 217-24.
74. Dogar, A.M., H. Towbin, and J. Hall, *Suppression of latent transforming growth factor (TGF)-beta1 restores growth inhibitory TGF-beta signaling through microRNAs.* J Biol Chem, 2011. **286**(18): p. 16447-58.
75. Ding, H., et al., *Characterization of the microRNA expression profile of cervical squamous cell carcinoma metastases.* Asian Pac J Cancer Prev, 2014. **15**(4): p. 1675-9.
76. Lu, J., et al., *MicroRNA expression profiles classify human cancers.* Nature, 2005. **435**(7043): p. 834-8.
77. Hudelist, G., et al., *cDNA array analysis of cytobrush-collected normal and malignant cervical epithelial cells: a feasibility study.* Cancer Genet Cytogenet, 2005. **158**(1): p. 35-42.
78. Lui, W.O., et al., *Patterns of known and novel small RNAs in human cervical cancer.* Cancer Res, 2007. **67**(13): p. 6031-43.
79. Wang, X., et al., *Aberrant expression of oncogenic and tumor-suppressive microRNAs in cervical cancer is required for cancer cell growth.* PLoS One, 2008. **3**(7): p. e2557.
80. Hermeking, H., *The miR-34 family in cancer and apoptosis.* Cell Death Differ, 2010. **17**(2): p. 193-9.
81. Wang, X., et al., *microRNAs are biomarkers of oncogenic human papillomavirus infections.* Proc Natl Acad Sci U S A, 2014.
82. Bandi, N., et al., *miR-15a and miR-16 are implicated in cell cycle regulation in a Rb-dependent manner and are frequently deleted or down-regulated in non-small cell lung cancer.* Cancer Res, 2009. **69**(13): p. 5553-9.
83. Lajer, C.B., et al., *The role of miRNAs in human papilloma virus (HPV)-associated cancers: bridging between HPV-related head and neck cancer and cervical cancer.* Br J Cancer, 2012. **106**(9): p. 1526-34.
84. Gillison, M.L., et al., *Human papillomavirus and diseases of the upper airway: head and neck cancer and respiratory papillomatosis.* Vaccine, 2012. **30 Suppl 5**: p. F34-54.
85. Qian, K., et al., *Identification and validation of human papillomavirus encoded microRNAs.* PLoS One, 2013. **8**(7): p. e70202.
86. Wei, J.S., et al., *microRNA profiling identifies cancer-specific and prognostic signatures in pediatric malignancies.* Clin Cancer Res, 2009. **15**(17): p. 5560-8.
87. Li, J., et al., *Improved RNA quality and TaqMan Pre-amplification method (PreAmp) to enhance expression analysis from formalin fixed paraffin embedded (FFPE) materials.* BMC Biotechnol, 2008. **8**: p. 10.
88. Ludyga, N., et al., *Nucleic acids from long-term preserved FFPE tissues are suitable for downstream analyses.* Virchows Arch, 2012. **460**(2): p. 131-40.
89. Hall, J.S., et al., *Enhanced stability of microRNA expression facilitates classification of FFPE tumour samples exhibiting near total mRNA degradation.* Br J Cancer, 2012. **107**(4): p. 684-94.

90. Patnaik, S.K., E. Kannisto, and S. Yendamuri, *Factors affecting the yield of microRNAs from laser microdissectates of formalin-fixed tissue sections.* BMC Res Notes, 2012. **5**: p. 40.
91. Clement-Ziza, M., et al., *Stabilization of RNA during laser capture microdissection by performing experiments under argon atmosphere or using ethanol as a solvent in staining solutions.* RNA, 2008. **14**(12): p. 2698-704.
92. Schuster, C., et al., *MicroRNA expression profiling of specific cells in complex archival tissue stained by immunohistochemistry.* Lab Invest, 2011. **91**(1): p. 157-65.
93. MMI. *MMI CellCut Plus*. 2014; Available from: http://www.molecular-machines.com/products/mmi_cellcut_plus/technology_27.
94. Vomelova, I., Z. Vanickova, and A. Sedo, *Methods of RNA purification. All ways (should) lead to Rome.* Folia Biol (Praha), 2009. **55**(6): p. 243-51.
95. Technologies, L. *The Basics: RNA Isolation*. 2014; Available from: http://www.lifetechnologies.com/no/en/home/references/ambion-tech-support/rna-isolation/general-articles/the-basics-rna-isolation.html.
96. Nelson, D.L.N.D.L.L.A.L.C.M.M., *Lehninger principles of biochemistry*. 2008, New York: W.H. Freeman.
97. *NanoDrop 2000/2000c Spectrophotometers - User manual* 2009; Available from: http://www.thermoscientific.com/en/search-results.html?matchDim=Y&keyword=nanodrop+2000%2F2000c+user+manual&activeTab=DOC&prdRefine=0&continueSearch=true.
98. Becker, C., et al., *mRNA and microRNA quality control for RT-qPCR analysis.* Methods, 2010. **50**(4): p. 237-43.
99. Tissot, C. *Analysis of miRNA content in total RNA preparations using the Agilent 2100 bioanalyzer (PDF)*. 2008 [cited 2011 20.04]; Available from: http://www.chem.agilent.com/search/?Ntt=performance+of+the+agilent+small+rna+assay.
100. Schroeder, A., et al., *The RIN: an RNA integrity number for assigning integrity values to RNA measurements.* BMC Mol Biol, 2006. **7**: p. 3.
101. Garzon, R., et al., *MicroRNA expression and function in cancer.* Trends Mol Med, 2006. **12**(12): p. 580-7.
102. Caldas, C. and J.D. Brenton, *Sizing up miRNAs as cancer genes.* Nat Med, 2005. **11**(7): p. 712-4.
103. Agilent Technologies, I., 2008, 2013. *Agilent Small RNA Kit Guide* 2013; Available from: http://www.chem.agilent.com/library/usermanuals/Public/G2938-90093_SmallRNA_KG_EN.pdf.
104. Butler, J.M., *Fundamentals of Forensic DNA Typing*. 2009, Elsevier Science. p. 130-31.
105. Dieffenbach, C.W., T.M. Lowe, and G.S. Dveksler, *General concepts for PCR primer design.* PCR Methods Appl, 1993. **3**(3): p. S30-7.
106. Bio-Rad. *Real-Time PCR Applications Guide*. 2006; Available from: http://www.gene-quantification.de/real-time-pcr-guide-bio-rad.pdf.
107. Jensen, S.G., et al., *Evaluation of two commercial global miRNA expression profiling platforms for detection of less abundant miRNAs.* BMC Genomics, 2011. **12**: p. 435.
108. Scientific, T.F. *Basic Principles of RT-qPCR*. Available from: http://www.thermoscientificbio.com/applications/basic-rt-qpcr/.
109. Butler, J.M., *Fundamentals of Forensic DNA Typing*. 2009, Elsevier Science. p. 119 - 121.
110. SIGMA-ALDRICH. *qPCR Technical Guide*. Available from: http://www.sigmaaldrich.com/content/dam/sigma-aldrich/docs/Sigma/General_Information/qpcr_technical_guide.pdf.
111. Bustin, S.A., et al., *The MIQE guidelines: minimum information for publication of quantitative real-time PCR experiments.* Clin Chem, 2009. **55**(4): p. 611-22.
112. Benes, V. and M. Castoldi, *Expression profiling of microRNA using real-time quantitative PCR, how to use it and what is available.* Methods, 2010. **50**(4): p. 244-9.

113. Jørgensen S, B.A., Møller S, Nielsen BS. *miRCURY LNA™ microRNA ISH Optimization Kit (FFPE) Instruction manual v2.0*. 2011; Available from: https://www.exiqon.com/ls/Documents/Scientific/miRCURY-LNA-microRNA-ISH-Optimization-Kit-manual.pdf.
114. Jorgensen, S., et al., *Robust one-day in situ hybridization protocol for detection of microRNAs in paraffin samples using LNA probes.* Methods, 2010. **52**(4): p. 375-81.
115. Nuovo, G.J., *In situ detection of precursor and mature microRNAs in paraffin embedded, formalin fixed tissues and cell preparations.* Methods, 2008. **44**(1): p. 39-46.
116. Nuovo, G.J., *In situ detection of microRNAs in paraffin embedded, formalin fixed tissues and the co-localization of their putative targets.* Methods, 2010. **52**(4): p. 307-15.
117. *Locked Nucleic Acid (LNA™) Technology*. Available from: http://www.exiqon.com/ls/PublishingImages/Figures/LNA-molecule.htm.
118. Bonin, S., et al., *Multicentre validation study of nucleic acids extraction from FFPE tissues.* Virchows Arch, 2010. **457**(3): p. 309-17.
119. Li, J., et al., *Comparison of miRNA expression patterns using total RNA extracted from matched samples of formalin-fixed paraffin-embedded (FFPE) cells and snap frozen cells.* BMC Biotechnol, 2007. **7**: p. 36.
120. Khan, A.A., et al., *MicroRNA-17~92 regulates effector and memory CD8 T-cell fates by modulating proliferation in response to infections.* Blood, 2013. **121**(22): p. 4473-83.
121. Wu, T., et al., *Temporal expression of microRNA cluster miR-17-92 regulates effector and memory CD8+ T-cell differentiation.* Proc Natl Acad Sci U S A, 2012. **109**(25): p. 9965-70.
122. Ballou, L.M. and R.Z. Lin, *Rapamycin and mTOR kinase inhibitors.* J Chem Biol, 2008. **1**(1-4): p. 27-36.

9 Appendix

9.1 Listed suppliers

Table 18. Listed chemicals, suppliers, suppliers home page

Chemicals	Supplier	URL
Absolute alcohol	Abus. Norway	
Xylene	Chemi-Teknik. Norway	http://chemi-teknik.no/1.html
Cresyl Violet acetate	Sigma-Aldrich. Missouri, USA	http://www.sigmaaldrich.com/chemistry.html
PBS tablets	Sigma-Aldrich. Missouri, USA	http://www.sigmaaldrich.com/chemistry.html
20x SSC buffer	Sigma-Aldrich. Missouri, USA	http://www.sigmaaldrich.com/chemistry.html
EDTA	Merck Millipore. Darmstadt, Germany.	http://www.merckmillipore.se/chemicals
NaCl	Sigma-Aldrich. Missouri, USA	http://www.sigmaaldrich.com/chemistry.html
KCl	Sigma-Aldrich. Missouri, USA	http://www.sigmaaldrich.com/chemistry.html
10x Maleic acid	Roche Diagnostics. Basel, Switzerland	http://www.roche.com/index.htm
Tris-HCl	Sigma-Aldrich. Missouri, USA	http://www.sigmaaldrich.com/chemistry.html
30 % BSA	Sigma-Aldrich. Missouri, USA	http://www.sigmaaldrich.com/chemistry.html
Tween-20	Dako (Agilent Technologies). California, USA	http://www.dako.com/no/
Rubber cement, Fixogum	MP Biomedicals. California, USA	http://www.mpbio.com/
Histokitt	Glasswarenfabrik. Sondheim, Germany	http://www.hecht-assistent.de/en/home.html
RNaseZap®	Life Technologies (Thermo Fisher Scientific). New York, USA	https://www.lifetechnologies.com/no/en/home.html
Sheep anti-DIG-	Roche	http://www.roche.com/index.htm

AP	Diagnostics. Basel, Switzerland	
Sheep serum	Jackson Immunoresearch. Pennsylvania, USA	http://www.jireurope.com/home/
NBT / BCIP tablets	Roche Diagnostics. Basel, Switzerland	http://www.roche.com/index.htm
Levamisol hydrochloride	Sigma-Aldrich. Missouri, USA	http://www.sigmaaldrich.com/chemistry.html
Nuclear Fast Red™	Sigma-Aldrich. Missouri, USA	http://www.sigmaaldrich.com/chemistry.html

Table 19. Listed; equipment, suppliers, suppliers home page.

Equipment	**Supplier**	**Home page**
MMI MembraneSlides, RNAse free	Molecular Machines & Industries (MMI). Zurich, Switzerland.	http://www.molecular-machines.com/home
MMI Isolation caps. Diffuser caps. 0.5ml	Molecular Machines & Industries (MMI). Zurich, Switzerland.	http://www.molecular-machines.com/home
MMI CellCut Plus	Molecular Machines & Industries (MMI). Zurich, Switzerland.	http://www.molecular-machines.com/home
Hybridiser HB-1D	Techne. Staffordshire, United Kingdom	http://www.techne.com/index.asp
OLYMPUS IX81F-3	OLYMPUS. Tokyo, Japan	http://www.olympus.no/
Pipet-lite L-20XLS, L-200XLS, L-1000XLS (LTS) manual pipette	Rainin Instruments (Mettler-Toledo).Greifensee, Switzerland	http://no.mt.com/no/no/home.html
BioClean tips Tips for LTS pipettes	Rainin Instruments (Mettler-Toledo). Greifensee, Switzerland	http://no.mt.com/no/no/home.html
Biosphere® SafeSeal Micro Tubes 1.5 ml, 2.0 ml.	SARSTEDT. Nümbrecht, Germany.	http://www.sarstedt.com/php/main.php
SafeSeal Micro Tubes 0.5 ml	SARSTEDT. Nümbrecht, Germany.	http://www.sarstedt.com/php/main.php
MS2 Minishaker	IKA. Stafen	http://www.ikausa.com/

(vortex)	Germany	
Microfuge® 18 Centrifuge	Beckman Coulter™. California, USA	https://www.beckmancoulter.com/wsrportal/wsr/index.htm
Thermo-Shaker PHMT (heating block)	Grant Instruments. Cambridge, United Kingdom	http://www2.grantinstruments.com/
NanoDrop 2000c Spectrophotometer	Thermo Fisher Scientific. New York, USA	http://www.no.fishersci.com/no/
2100 Bioanalyzer	Agilent Technologies. California, USA	http://www.home.agilent.com/agilent/home.jspx?cc=US&lc=eng
PCR Strip tubes (0.2 ml Thin Wall Clear) w/PCR Strip caps	Axygen Scientific Inc. California, USA	http://www.corning.com/lifesciences/us_canada/en/products/axygen.aspx
ThermoStat plus MTP (heating block)	Eppendorf. Hamburg, Germany	http://www.eppendorf.com/NC-en/
Galaxy Mini Centrifuge	VWR International. Pennsylvania, USA	https://no.vwr.com/app/Home
LightCycler® 480 Multiwell Plate 96 w/sealing foil	Roche Diagnostics. Basel, Switzerland	http://www.roche.com/index.htm
LightCycler® 480	Roche Diagnostics. Basel, Switzerland	http://www.roche.com/index.htm
Weight scale	Mettler Toledo. Greifensee, Switzerland	http://no.mt.com/no/no/home.html
Dako Pen	Dako (Agilent Technologies). California, USA	http://www.dako.com/no/
StatSpin Hybridizer	Dako (Agilent Technologies). California, USA	http://www.dako.com/no/
Milli-Q gradient, Elix and Biopac	Merck Millipore. Darmstadt, Germany	http://www.merckmillipore.com/
SuperFrost Plus®	Menzel (Thermo Fisher Scientific). Braunschweig, Germany	http://www.menzel.de/

Table 20. Listed; Kits, suppliers, suppliers home page.

Kit	**Supplier**	**Home page**
High Pure FFPET RNA isolation kit	Roche Diagnostics. Basel, Switzerland	http://lifescience.roche.com/shop/products/high-pure-ffpet-rna-isolation-kit#tab-0

MiRNeasy FFPE kit protocol	Qiagen. Venlo, Netherland	http://www.qiagen.com/products/catalog/sample-technologies/rna-sample-technologies/miRNA/mirneasy-ffpe-kit
Agilent Small RNA kit	Agilent Technologies. California, USA	http://www.home.agilent.com/agilent/home.jspx?cc=US&lc=eng
Universal cDNA synthesis kit	Exiqon. Vedbaek, Denmark	http://www.exiqon.com/miRNA-pcr-kits
SYBR Green master mix, Universal RT, 2.5 ml	Exiqon. Vedbaek, Denmark.	http://www.exiqon.com/miRNA-pcr-kits
Reference gene primer sets (miR-23a, miR-191, miR-18a, miR-18b)	Exiqon. Vedbaek, Denmark	http://www.exiqon.com/miRNA-pcr-controls
miRCURY LNA™ miRNAISH optimization kit (FFPE)	Exiqon. Vedbaek, Denmark	http://www.exiqon.com/miRNA-ish-kit
LNA™ miRNAprobe, double-DIG labeled (miR-18a, miR-18b)	Exiqon. Vedbaek, Denmark	http://www.exiqon.com/microrna-In-situ-Hybridization-detection-probes

9.2 Raw data

9.2.1 RNA concentrations and Cq values of microdissected test samples

Table 21 show a comparison between miRNeasy FFPE kit from Qiagen and High Pure FFPET RNA isolation kit from Roche.

Laser microdissection				Nanodrop RNA			C_q values miR-191			C_q values miR-23a			C_q values Spike-in		
Date	Name	Section	Method	ng/µl	260/280	260/230	1	2	Mean	1	2	Mean	1	2	Mean
19.9.13	59	E	Qiagen	5.40	1.75	0.54	29.87	30.53	30.20				12.33	6.30	9.32
	59	E	Roche	11.80	1.61	0.57	35.55	35.6	35.58				12.83	11.22	12.03
	59	S	Qiagen	4.40	1.57	0.31	31.72	32.69	32.21				12.59	12.72	12.66
	59	S	Roche	12.50	1.60	0.62	0.00	34.65	34.65				11.68	13.62	12.65
	MCF						23.14	21.65	22.40				12.54	12.51	12.53
	noRT						0.00	0.00	0.00				0.00	0.00	0.00
	noTC						0.00	0.00	0.00				0.00	0.00	0.00

Table 22 shows the laser microdissected samples extracted with miRNeasy FFPE kit. Modification of the standard protocol was performed. Samples were either incubated at 56 ˚C for 1 hour (1h) or at 56 ˚C overnight (O/N). Spike-in is used as positive control. The different concentrations in the spike in control is due to a new batch diluted with 50 % less MQ- water than used in the first dilution (recommended in the miRNeasy FFPE kit).

Laser microdissection				Nanodrop RNA			C_q values miR-191			C_q values miR-23a			C_q values Spike-in		
Date	Name	Section	Method	ng/µl	260/280	260/230	1	2	Mean	1	2	Mean	1	2	Mean
28.11.13	139	E	Qiagen	33.10	1.18	0.34	35.32	33.14	34.23	34.53	33.94	34.24	14.66	14.77	14.72
	139	S	Qiagen	26.70	1.11	0.29	32.02	33.88	32.95	31.34	32.32	31.83	15.03	15.28	15.16
	170	E	Qiagen	42.40	1.20	0.36	35.77	0.00	35.77	35.06	35.48	35.27	15.23	15.68	15.46
	170	S	Qiagen	18.10	1.10	0.25	32.12	33.72	32.92	31.51	32.18	31.85	16.68	15.82	16.25
	232	E	Qiagen	80.00	1.31	0.43	36.55	0.00	36.55	35.72	35.95	35.84	0.00	0.00	0.00
	232	S	Qiagen	10.40	0.88	0.16	29.79	31.27	30.53	28.01	28.99	28.50	0.00	15.95	7.98
	252	E	Qiagen	38.80	1.15	0.33	35.09	33.75	34.42	35.54	35.96	35.75	14.84	14.84	14.84
	252	S	Qiagen	19.80	1.09	0.26	0.00	0.00	0.00	0.00	0.00	0.00	14.69	14.84	14.77
	MCF						26.33	26.36	26.35	27.26	27.30	27.28	14.75	14.97	14.86
	noRT						0.00	0.00	0.00	0.00	0.00	0.00	0.00	0.00	0.00
	noTC						0.00	0.00	0.00	0.00	0.00	0.00	0.00	0.00	0.00
19.12.13	91	E	Qiagen	5.20	1.45	0.57	31.26	32.20	31.73	29.57	30.94	30.26	0.00	0.00	0.00
	91	S	Qiagen	2.00	1.45	0.31	31.98	32.60	32.29	31.13	32.68	31.91	0.00	0.00	0.00
	136	E	Qiagen	3.00	1.64	0.59	30.30	30.48	30.48	29.83	29.89	29.86	24.47	23.66	24.07
	136	S	Qiagen	3.30	1.75	0.36	33.10	32.88	32.88	32.40	32.38	32.39	24.11	24.12	24.12
	164	E	Qiagen	3.70	1.50	0.65	31.67	31.65	31.65	31.60	31.95	31.78	22.95	22.91	22.93
	164	S	Qiagen	7.00	1.52	0.65	31.46	31.39	31.39	31.48	31.71	31.60	23.62	23.34	23.48
	MCF						28.24	28.36	28.36	29.21	29.25	29.23	23.97	23.80	23.89
	noRT						0.00	0.00	0.00	0.00	0.00	0.00	0.00	0.00	0.00
	noTC						0.00	0.00	0.00	0.00	0.00	0.00	0.00	0.00	0.00
17.1.14	166	E1_1h	Qiagen	3.50	1.84	0.57	30.25	29.76	29.76	29.86	29.88	29.87	24.00	23.79	23.90
	166	E_O/N	Qiagen	-	-	-	30.79	31.04	31.04	30.08	30.49	30.29	23.45	23.50	23.48
	166	S_1h	Qiagen	4.00	1.69	0.37	31.77	31.66	31.66	32.23	31.98	32.11	23.67	23.47	23.57
	166	S_O/N	Qiagen	-	-	-	36.52	0.00	36.52	35.54	35.44	35.49	23.45	23.50	23.48
	178	E_1h	Qiagen	2.30	1.53	0.39	32.18	32.59	32.59	32.46	31.75	32.11	24.18	24.06	24.12
	178	E_O/N	Qiagen	-	-	-	33.17	32.55	32.55	32.83	34.11	33.47	22.08	22.24	22.16
	178	S_1h	Qiagen	2.30	1.47	0.44	33.59	33.30	33.30	33.63	33.26	33.45	22.55	22.39	22.47
	178	S_O/N	Qiagen	-	-	-	34.57	34.49	34.49	34.02	34.30	34.16	22.53	22.54	22.54
	MCF		Qiagen				27.22	27.12	27.12	27.89	27.97	27.93	22.13	22.08	22.11
	noRT		Qiagen				0.00	0.00	0.00	0.00	0.00	0.00	0.00	0.00	0.00
	noTC		Qiagen				0.00	0.00	0.00	0.00	0.00	0.00	0.00	0.00	0.00

9.2.2 RNA concentrations and Cq values of macrodissected test samples

Table 23 shows the RNA concentrations of macrodissected tissue. Spike-in is used as positive control.

Histological section				Nanodrop RNA			C_q values miR-23a			C_q values Spike-in		
Date	Sample	Section	Method	ng/µl	260/280	260/230	1	2	Mean	1	2	Mean
21.1.14												
	29	Normal	Qiagen	28.40	1.83	0.66	26.78	26.78	26.78	22.93	22.75	22.84
	34	Normal	Qiagen	24.40	1.84	0.86	26.85	26.91	26.88	23.77	23.67	23.72
	101	CIN3	Qiagen	16.50	1.81	1.05	27.82	27.77	27.80	22.71	22.15	22.43
	145	CIN3	Qiagen	19.00	1.88	1.21	26.85	26.39	26.62	22.84	21.95	22.40
	166	CIN3	Qiagen	20.70	1.87	1.05	27.23	27.38	27.31	22.86	23.10	22.98
	178	CIN3	Qiagen	14.10	1.69	0.77	27.02	27.30	27.16	0.00	0.00	0.00
	MCF		Qiagen				28.99	28.96	28.98	21.75	21.83	21.79
	noRT		Qiagen				0.00	0.00	0.00	0.00	0.00	0.00
	noTC		Qiagen				0.00	0.00	0.00	0.00	0.00	0.00

9.2.3 RNA concentrations and Cq values of project samples

Table 24 shows the RNA concentrations of macrodissected tissue.

Project samples				Nanodrop RNA			C_q values miR 191				C_q values miR 23a			
Date	Name	Section	Method	ng/µl	260/280	260/230	1	2	3	Mean	1	2	3	Mean
12.2.14	001	Normal	Qiagen	13.60	2.00	1.22	29.00	28.89		28.95	27.45	27.75		27.60
	008	Normal	Qiagen	17.30	1.81	1.11	28.84	28.91		28.88	28.07	28.48		28.28
	034	Normal	Qiagen	24.40	1.84	0.86	27.86	27.96		27.91	26.92	26.96		26.94
	139	CIN3	Qiagen	27.70	1.97	1.38	27.78	28.07		27.93	28.06	27.83		27.95
	164	CIN3	Qiagen	44.20	1.94	1.68	28.42	28.47		28.45	27.84	27.63		27.74
	252	CIN3	Qiagen	39.90	1.87	1.56	28.51	28.40		28.46	28.36	28.19		28.28
	MCF						27.89	27.90		27.90	29.09	29.06		29.08
	noRT						0.00	0.00		0.00	0.00	0.00		0.00
	noTC						0.00	0.00		0.00	0.00	0.00		0.00
12.2.14	004	Normal	Qiagen	68.70	1.90	1.61	27.84	28.17		28.01	27.15	27.19		27.17
	029	Normal	Qiagen	28.40	1.83	0.66	27.86	27.70		27.78	27.26	27.29		27.28
	063	Normal	Qiagen	11.20	1.88	1.45	28.38	28.25		28.32	27.21	27.38		27.30
	136	CIN3	Qiagen	20.30	1.90	1.46	28.79	28.42		28.61	28.65	28.77		28.71
	170	CIN3	Qiagen	25.20	1.79	1.33	29.18	28.99		29.09	31.06	30.64		30.85
	182	CIN3	Qiagen	14.40	1.94	1.63	29.03	28.95		28.99	29.56	28.51		29.04
	MCF						27.95	27.97		27.96	29.41	29.81		29.61
	noRT						0.00	0.00		0.00	0.00	0.00		0.00
	noTC						0.00	0.00		0.00	0.00	0.00		0.00
19.2.14	064	Normal	Qiagen	21.80	1.95	1.34	27.84	27.96	28.26	28.02	27.24	27.49	27.39	27.37

	073	Normal	Qiagen	12.10	1.97	0.99	28.26	28.28	28.48	28.34	27.71	27.78	27.70	27.73
	020	CIN3	Qiagen	48.40	1.93	1.49	28.00	27.78	27.73	27.84	27.76	27.56	27.51	27.61
	075	CIN3	Qiagen	29.50	1.97	1.98	27.74	28.14	27.81	27.90	28.18	28.24	28.14	28.19
	126	CIN3	Qiagen	21.90	1.77	0.88	28.53	28.96	28.99	28.83	28.63	28.60	28.40	28.54
	MCF						27.40	27.26	27.34	27.33	29.21	29.09	29.21	29.17
	noRT						0.00	0.00	0.00	0.00	0.00	0.00	0.00	0.00
	noTC						0.00	0.00	0.00	0.00	0.00	0.00	0.00	0.00
24.2.14	077	Normal	Qiagen	38.50	1.96	1.44	27.43	27.49	27.35	27.42	26.91	26.91	26.66	26.83
	092	Normal	Qiagen	39.80	1.94	1.42	27.60	27.57	27.98	27.72	26.94	26.84	26.74	26.84
	118	Normal	Qiagen	32.30	1.94	0.84	27.95	27.86	27.99	27.93	27.43	27.41	27.41	27.42
	016	CIN3	Qiagen	69.00	1.98	1.91	27.71	27.77	27.58	27.69	28.03	27.92	27.87	27.94
	080	CIN3	Qiagen	16.80	2.08	1.29	28.44	27.84	28.45	28.24	28.92	28.63	28.59	28.71
	MCF						27.42	26.98	27.11	27.17	29.60	29.38	29.33	29.44
	noRT						0.00	0.00	0.00	0.00	0.00	0.00	0.00	0.00
	noTC						0.00	0.00	0.00	0.00	0.00	0.00	0.00	0.00
27.2.14	060	CIN3	Qiagen	19.70	1.79	1.36	27.33	27.48	27.52	27.44	27.00	27.51	0.00	27.26
	109	Normal	Qiagen	37.50	1.89	1.61	27.66	28.24	28.73	28.21	25.43	26.75	0.00	26.09
	147	Normal	Qiagen	31.80	1.90	1.63	27.51	27.58	27.57	27.55	26.96	27.16	26.87	27.00
	159	CIN3	Qiagen	11.20	1.81	1.21	27.46	27.39	27.40	27.42	27.76	27.66	27.74	27.72
	160	Normal	Qiagen	16.20	1.82	1.16	27.95	28.12	27.93	28.00	27.86	27.89	27.72	27.82
	MCF						26.40	26.24	26.50	26.38	28.49	28.39	28.40	28.43
	noRT						0.00	0.00	0.00	0.00	0.00	0.00	0.00	0.00
	noTC						0.00	0.00	0.00	0.00	0.00	0.00	0.00	0.00
4.3.14	121	Normal	Qiagen	13.30	2.01	1.29	28.18	28.34	28.11	28.21	26.93	26.92	27.13	26.99
	186	CIN3	Qiagen	51.20	1.94	1.66	27.44	27.59	27.45	27.49	27.18	27.20	27.20	27.19
	171	CIN3	Qiagen	20.4	1.89	1.51	27.53		27.46	27.50	27.41	27.21	27.27	27.30
	214	CIN3	Qiagen	14.80	2.04	0.95	28.19	28.22	28.51	28.31	27.90	28.23	27.97	28.03
	217	CIN3	Qiagen	24.70	1.96	1.16	28.42	28.40	28.53	28.45	28.67	28.13	28.15	28.32
	MCF						26.99	26.82	27.29	27.03	28.54	27.59		28.07
	noRT						0.00	0.00	0.00	0.00	0.00	0.00	0.00	0.00
	noTC						0.00	0.00	0.00	0.00	0.00	0.00	0.00	0.00
6.3.14	035	CIN3	Qiagen	51.00	1.87	1.65	27.70	27.63	27.75	27.69	29.18	29.01	29.11	29.10
	211	CIN3	Qiagen	14.00	1.73	1.18	27.88	27.96	28.18	28.01	29.08	29.30	29.05	29.14
	081	CIN3	Qiagen	8.30	1.77	1.10	27.82	27.84	28.00	27.89	28.91	29.27	29.19	29.12
	251	Normal	Qiagen	15.70	1.77	1.22	27.20	27.38	27.31	27.30	28.52	28.55	28.67	28.58
	184	Normal	Qiagen	28.00	1.81	1.45	27.81	27.94	28.01	27.92	28.43	28.53	28.52	28.49
	MCF						26.21	26.23	26.30	26.25	29.01	29.08	28.89	28.99
	noRT						0.00	0.00	0.00	0.00	0.00	0.00	0.00	0.00
	noTC						0.00	0.00	0.00	0.00	0.00	0.00	0.00	0.00

28.3.14	181	CIN3	Qiagen	27.30	2.00	1.84	27.39	27.52	27.66	27.52	24.42	24.43	24.50	24.45
	247	Normal	Qiagen	19.60	1.86	1.16	27.88	28.13	27.96	27.99	24.39	24.13	24.15	24.22
	MCF						29.81	30.39	30.49	30.23	27.78	27.63	27.57	27.66
	noRT						0.00	0.00	0.00	0.00	0.00	0.00	0.00	0.00
	noTC						0.00	0.00	0.00	0.00	0.00	0.00	0.00	0.00

Table 25 shows the miR-18a and miR-18b concentrations of macrodissected sections.

Project samples				C_q values miR-18a				C_q values miR-18b			
Date	Name	Section	Method	parallel 1	parallel 2	parallel 3	Mean	parallel 1	parallel 2	parallel 3	Mean
12.2.14	001	Normal	Qiagen	32.44	32.29		32.37	32.58	32.88		32.73
	008	Normal	Qiagen	31.93	31.71		31.82	32.76	32.69		32.73
	034	Normal	Qiagen	31.49	31.01		31.25	31.51	31.66		31.59
	139	CIN3	Qiagen	31.90	32.36		32.13	32.00	32.01		32.01
	164	CIN3	Qiagen	30.94	31.00		30.97	31.47	31.03		31.25
	252	CIN3	Qiagen	31.88	30.93		31.41	31.37	31.13		31.25
	MCF			29.82	29.90		29.86	30.24	30.39		30.32
	noRT			0.00	0.00	0.00	0.00	0.00	0.00	0.00	0.00
	noTC			0.00	0.00	0.00	0.00	0.00	0.00	0.00	0.00
12.2.14	004	Normal	Qiagen	32.11	32.39		32.25	31.68	33.05		32.37
	029	Normal	Qiagen	32.63	31.85		32.24	32.29	31.76		32.03
	063	Normal	Qiagen	31.43	31.83		31.63	31.64	31.87		31.76
	136	CIN3	Qiagen	31.68	31.90		31.79	31.95	31.77		31.86
	170	CIN3	Qiagen	33.88	32.98		33.43		33.79		33.79
	182	CIN3	Qiagen	32.09	32.70		32.40	32.52	32.44		32.48
	MCF			29.75	29.99		29.87	30.24	30.03		30.14
	noRT			0.00	0.00	0.00	0.00	0.00	0.00	0.00	0.00
	noTC			0.00	0.00	0.00	0.00	0.00	0.00	0.00	0.00
19.2.14	064	Normal	Qiagen	31.65	32.15	31.46	31.75	32.32	31.99	31.65	31.99
	073	Normal	Qiagen	32.40	32.52	33.15	32.69	32.47	32.22	32.35	32.35
	020	CIN3	Qiagen	29.57	31.94	31.28	30.93	31.90	31.70	32.72	32.11
	075	CIN3	Qiagen	31.82	32.02	31.98	31.94	31.99	32.43	31.80	32.07
	126	CIN3	Qiagen	31.86	31.07	30.92	31.28	31.34	31.73	31.51	31.53
	MCF			29.80	29.36	29.72	29.63	29.67	29.89	29.98	29.85
	noRT			0.00	0.00	0.00	0.00	0.00	0.00	0.00	0.00
	noTC			0.00	0.00	0.00	0.00	0.00	0.00	0.00	0.00
24.2.14	077	Normal	Qiagen	31.39	30.81	31.48	31.23	31.08	30.95	31.60	31.21
	092	Normal	Qiagen	31.24	31.44	31.20	31.29	31.62	31.99	31.41	31.67
	118	Normal	Qiagen	31.40	31.76	31.66	31.61	31.61	31.39	31.94	31.65
	016	CIN3	Qiagen	30.56	30.49	30.16	30.40	30.83	30.87	30.82	30.84

	080	CIN3	Qiagen	31.40	31.53	31.54	31.49	31.67	32.00	32.44	32.04
	MCF			29.47	29.30	29.47	29.41	29.45	29.67	29.56	29.56
	noRT			0.00	0.00	0.00	0.00	0.00	0.00	0.00	0.00
	noTC			0.00	0.00	0.00	0.00	0.00	0.00	0.00	0.00
27.2.14	060	CIN3	Qiagen	31.65	31.73	31.52	31.63	31.56	31.79	31.63	31.66
	109	Normal	Qiagen	31.29	32.25	32.15	31.90	31.71	33.11	32.58	32.47
	147	Normal	Qiagen	30.94	30.50	30.47	30.64	31.20	30.71	31.12	31.01
	159	CIN3	Qiagen	30.64	30.47	30.49	30.53	30.64	30.42	30.59	30.55
	160	Normal	Qiagen	31.25	31.53	31.23	31.34	30.97	31.56	30.97	31.17
	MCF			29.03	28.70	28.82	28.85	29.39	28.86	29.33	29.19
	noRT			0.00	0.00	0.00	0.00	0.00	0.00	0.00	0.00
	noTC			0.00	0.00	0.00	0.00	0.00	0.00	0.00	0.00
4.3.14	121	Normal	Qiagen	31.69	31.44	31.74	31.62	31.72	31.18	32.67	31.86
	186	CIN3	Qiagen	30.48	30.46	30.14	30.36	29.98	30.60	31.16	30.58
	171	CIN3	Qiagen	31.59	31.88	31.72	31.73	31.64	31.84	32.01	31.83
	214	CIN3	Qiagen	31.84	30.93	32.22	31.66	31.26	31.91	32.24	31.80
	217	CIN3	Qiagen	32.30	31.92	31.72	31.98	31.88	32.45	31.82	32.05
	MCF			29.27	29.21	29.23	29.24	29.93	29.26	29.47	29.55
	noRT			0.00	0.00	0.00	0.00	0.00	0.00	0.00	0.00
	noTC			0.00	0.00	0.00	0.00	0.00	0.00	0.00	0.00
6.3.14	035	CIN3	Qiagen	31.70	31.45	31.54	31.56	31.66	31.72	31.44	31.61
	211	CIN3	Qiagen	31.40	32.00	31.44	31.61	31.40	31.68	31.33	31.47
	081	CIN3	Qiagen	31.60	31.25	31.72	31.52	31.55	31.30	31.84	31.56
	251	Normal	Qiagen	31.80	31.96	31.48	31.75	31.52	31.78	32.04	31.78
	184	Normal	Qiagen	31.73	31.86	32.20	31.93	33.08	31.82	32.15	32.35
	MCF			28.75	28.66	28.79	28.73	28.78	28.68	29.01	28.82
	noRT			0.00	0.00	0.00	0.00	0.00	0.00	0.00	0.00
	noTC			0.00	0.00	0.00	0.00	0.00	0.00	0.00	0.00
28.3.14	181	CIN3	Qiagen	31.00	30.82	31.17	31.00	30.98	31.31	31.21	31.17
	201	Normal	Qiagen	0	0	0	0	0	0	0	0
	213	Normal	Qiagen	0	36.39	0	36.39	35.48	36.03	0	35.76
	247	Normal	Qiagen	31.31	31.56	31.75	31.54	31.77	31.24	31.49	31.50
	MCF			32.05	33.24	33.37	32.89	33.77	32.76	33.88	33.47
	noRT			0.00	0.00	0.00	0.00	0.00	0.00	0.00	0.00
	noTC			0.00	0.00	0.00	0.00	0.00	0.00	0.00	0.00

9.2.4 MiRNA concentrations

Table 26 shows results obtained from Bioanalyzer 2100.

29* (Normal tissue)	
Small RNA Concentration[pg/µl]:	4 745,2
miRNA Concentration[pg/µl]:	2 075,6
miRNA / Small RNA Ration [%]:	44
Result Flagging Label:	44 %
miRNA; Concentration:	2075.60 pg/µl
34* (Normal tissue)	
Small RNA Concentration[pg/µl]:	11798,3
miRNA Concentration[pg/µl]:	5271,2
miRNA / Small RNA Ration [%]:	45
Result Flagging Label:	45 %
miRNA; Concentration:	5271.20 pg/µl
001* (Normal tissue)	
Small RNA Concentration[pg/µl]:	4599,9
miRNA Concentration[pg/µl]:	2485,4
miRNA / Small RNA Ration [%]:	54
Result Flagging Label:	54 %
miRNA; Concentration:	2485.40 pg/µl
008* (Normal tissue)	
Small RNA Concentration[pg/µl]:	5011,6
miRNA Concentration[pg/µl]:	1884,4
miRNA / Small RNA Ration [%]:	38
Result Flagging Label:	38 %
miRNA; Concentration:	1884.40 pg/µl
004* (Normal tissue)	
Small RNA Concentration[pg/µl]:	21747,6
miRNA Concentration[pg/µl]:	7790,5
miRNA / Small RNA Ration [%]:	36
Result Flagging Label:	36 %
miRNA; Concentration:	7790.50 pg/µl
63* (Normal tissue)	
Small RNA Concentration[pg/µl]:	4641,1
miRNA Concentration[pg/µl]:	2113,5
miRNA / Small RNA Ration [%]:	46
Result Flagging Label:	46 %
miRNA; Concentration:	2113.50 pg/µl
164 (CIN3)	
Small RNA Concentration[pg/µl]:	13154,9
miRNA Concentration[pg/µl]:	4175,0
miRNA / Small RNA Ration [%]:	32
Result Flagging Label:	32 %
miRNA; Concentration:	4175 pg/µl
252 (CIN3)	
Small RNA Concentration[pg/µl]:	11896,8
miRNA Concentration[pg/µl]:	4385,4
miRNA / Small RNA Ration [%]:	37
Result Flagging Label:	37 %

miRNA; Concentration:	4385.40 pg/µl
126 (CIN3)	
Small RNA Concentration[pg/µl]:	4368,9
miRNA Concentration[pg/µl]:	1623,5
miRNA / Small RNA Ration [%]:	37
Result Flagging Label:	37 %
miRNA; Concentration:	1623.50 pg/µl
75 (CIN3)	
Small RNA Concentration[pg/µl]:	423375,9
miRNA Concentration[pg/µl]:	77852,3
miRNA / Small RNA Ration [%]:	18
Result Flagging Label:	18 %
miRNA; Concentration:	77852.20 pg/µl

9.2.5 Visualization of miR-18a and miR-18b in CISH

Table 27 shows semi-quantitative scoring of CISH positives.

Proj.no.	CIN3 miR-18a	Normal miR-18a	CIN3 miR-18b	Normal miR-18b
16	17	2	15	2
20	27	0	31	2
35	43	1	38	3
60	35	0	12	2
75	21	1	32	1
80	29	2	24	7
81	27	2	22	3
126	51	0	50	0
136	39	0	40	2
139	6	3	13	4
159	35	1	37	0
164	52	N/A	53	N/A
170	75	3	73	2
181	13	N/A	38	N/A
182	2	1	9	1
186	44	7	36	7
211	16	0	19	3
214	5	0	6	2
217	27	1	20	0
252	70	1	130	2